

Phytoplankton community shift in response to experimental Cu addition at the elevated CO₂ levels (Arabian Sea, winter monsoon)

Diksha Sharma^{1,2}, Haimanti Biswas^{1,3*}, Mintu Chowdhury^{1,4}, Saumya Silori^{1,3}, Medhavi Pandey^{1,3}, and Durbar Ray¹

¹CSIR National Institute of Oceanography, Biological Oceanography Division, Dona Paula, Goa 403004, India

²Affiliated for Ph.D. under Bharathidasan University, Tiruchirappalli, Tamil Nadu 620024, India

³Academy of Scientific and Innovative Research (AcSIR), Ghaziabad-201002, India

⁴School of Oceanographic Studies, Jadavpur University, Kolkata 700032, India

* Corresponding author: haimanti.biswas@nio.org; haimanti.biswas.nio@gmail.com

Abstract

Understanding phytoplankton community shifts under multiple stressors is becoming increasingly important. Among other combinations of stressors, the impact of trace metal toxicity on marine phytoplankton under the ocean acidification scenario is an important aspect to address. Such multiple stressor studies are rare from the Arabian Sea, one of the highest productive oceanic provinces within the North Indian Ocean. We studied the interactive impacts of copper (Cu) and CO₂ enrichment on two natural phytoplankton communities from the eastern and central Arabian Sea. Low dissolved silicate (DSi < 2 μM) favoured smaller diatoms (e. g *Nitzschia* sp.) and non-diatom (*Phaeocystis*). CO₂ enrichment caused both positive (*Nitzschia* sp. and *Phaeocystis* sp.) and negative (*Cylindrotheca closterium*, *Navicula* sp., *Pseudo-nitzschia* sp., *Alexandrium* sp., and *Gymnodinium* sp.) growth impacts. The addition of Cu under the ambient CO₂ level (A-CO₂) hindered cell division in most of the species, whereas, Chl_a contents were nearly unaffected. Interestingly, CO₂ enrichment seemed to alleviate Cu toxicity in some species (*Nitzschia* sp., *Cylindrotheca closterium*, *Guinardia flaccida*, and *Phaeocystis*) and increased their growth rates. This could be related to the cellular Cu demand and energy budget at elevated CO₂ levels. Dinoflagellates were more sensitive to Cu supply compared to diatoms and prymnesiophytes and could be related to the unavailability of prey. Such community shifts in response to the projected ocean acidification, oligotrophy, and Cu pollution may impact trophic transfer and carbon cycling in this region.

Keywords: Arabian Sea; Copper; Toxicity; Phytoplankton; Ocean acidification; Pennate diatom; *Phaeocystis*.

1.Introduction

Trace metals like iron (Fe), copper (Cu), zinc (Zn), manganese (Mn), cadmium (Cd) act as a cofactor for several metalloenzymes (Twining et al. 2013) that are involved in important biochemical processes. These trace elemental cycles and marine phytoplankton seemed to have co-evolved in the oceans (Morel 2008). Substantial uptake of these metals by marine phytoplankton was evident in many studies (Sunda 2012; Mellett et al. 2018). Among other trace metals, Cu is highly reactive and usually available in multiple oxidation states which controls its solubility, binding strength with ligands, and biological availability (Sunda 2012). Cu limitation may severely impact some of the key cellular biochemical processes in marine diatoms (Kong and Price 2020). However, at higher levels, Cu can be highly toxic for marine phytoplankton (Lopez et al. 2019). Most of the Cu present in the dissolved form is usually chelated with organic ligands and <1% is available as free Cu ions (Coale and Bruland 1990; Moffet and Dupont 2007). In seawater, the other metal ions like Zn with a lower stability complex can be outcompeted by Cu ions and may hinder chelation with particulates followed by an extension of the residence time of Cu in the sea (Irving and William 1953). Hydrogen ion (H⁺) concentration in the surface ocean can directly alter trace metal bioavailability, and toxicity (Shi et al. 2010).

The oceans absorbed approximately 25% of CO₂ emitted to the atmosphere from anthropogenic sources (De Vries et al. 2017). The CO₂ injection into the surface ocean is altering the carbon chemistry and consequently, the average pH has already decreased by 0.1 unit from pre-industrial times (Ocean acidification; OA) (Sabine et al. 2004; Raven et al. 2005). The CO₂ concentration is expected to increase up to ≈900 μatm by 2100 if anthropogenic emissions are not restricted (IPCC, 2020). And a corresponding decrease in surface seawater pH is expected in the future ocean (Doney et al. 2009). One of the profound impacts of changing carbon chemistry can be on trace metal speciation (Stockdale et al. 2016). OA is likely to cause substantial enhancement in the concentrations of free trace metal ions in marine waters (Millero et al. 2009) and at elevated concentrations, most of the trace metals can be potentially lethal for marine organisms.

OA was found to directly impact metal (Cu, Cd) uptake and release by marine diatoms (Liu et al. 2016). Shi et al. (2010) noticed that the biological uptake of Fe by marine phytoplankton decreased under OA. Recently in some studies, it was noticed that OA helped to ameliorate metal toxicity (Cd) in two marine diatoms (Dong et al. 2020a; 2020b). These studies showed that at the elevated CO₂ levels, the model marine diatoms were able to upregulate certain genes involved in some biochemical synthesis that was likely to help in reducing the metal toxicity. Reduced nutrient supply, particularly DSi significantly impacted metal tolerance and adsorption capacity in a model marine

diatom (Zhou et al. 2020). Therefore, in the future, the increasing CO₂ levels, along with trace metals enrichment may have considerable impacts on the phytoplankton community and carbon cycling. However, the combination of multiple stressors such as trace metals and OA has received very little attention (Millero et al. 2009; Shi et al. 2010).

In the coastal waters, there could be land-driven direct sources of metals like Cu from fluvial input, upwelling waters, and anthropogenic sources like antifouling paints. But interestingly, a significant amount of Cu can be leached from the aerosol in the seawater (Mahowald et al. 2018) and was seen to impact the phytoplankton community (Paytan et al. 2009; Jordi et al. 2012). The primary sources of Cu in the aerosol are the burning of fossil fuel, tires, and metal smelting (Eichler et al. 2014) are very prominent in industrially developed countries (Tian et al. 2015). This is to be noted that an almost equal amount of Cu can be added to the oceans by atmospheric deposition as compared to the fluvial input and upwelling waters (Takano et al. 2014). The Arabian Sea is a dynamic and productive oceanic area that is highly influenced by the monsoon wind and its reversal. Particularly, certain areas of the Arabian Sea receive a large volume of atmospheric dust (Pease et al. 1998) which directly supports high phytoplankton production (Liao et al. 2016). Pease et al (1998) reported the highest level of dust concentration over the northeastern Arabian Sea (63°-68°) during the winter monsoon. Therefore, the oceanic areas that experience considerable dust deposition, may likely be exposed to higher trace metal fluxes. Consequently, the phytoplankton from this area may face toxic impacts (Paytan et al. 2009; Jordi et al. 2012). Moffett et al. (2015) noticed enhanced growth of some phytoplankton genera in response to Cu addition from the Central Arabian Sea and indicated that certain species might have higher Cu tolerance. Likewise, Neethu et al. (2021) conducted a study on two estuarine diatom species isolated from the Cochin estuary, southwest coast of India and reported high Cu tolerance, though the interspecific response differed significantly. Such quality may play a key role in the phytoplankton community shift in this region. Further, the Arabian Sea has also been identified as a perennial source of atmospheric CO₂ and usually displays higher *p*CO₂ (>400 μatm) in the surface waters (Sarma et al. 1998; Sarma 2003 and Valsala et al. 2021). Such a combination of naturally occurring high *p*CO₂ levels as well as atmospheric deposition may have potential impacts on the natural phytoplankton community from this region. However, whether the OA and Cu stress combinedly can act in a synergistic or antagonistic way, is not clear yet, and such studies are rare in this area. There is only one study (Sharma et al. 2020) from the Indian shelf water (10.52°N, 75.16°E) documenting the responses of phytoplankton assemblage to the addition of Zn and Cu under simulated OA during the southwest monsoon. It was revealed that certain phytoplankton species can be highly resistant or sensitive under the combined stress of metal ions and low pH and

thus may lead to the community shift. Furthermore, this experiment was conducted on a simulated diatom bloom under nutrient enrichment. And during the southwest monsoon, upwelling occurs in this region, and the phytoplankton are expected to be familiar with high $p\text{CO}_2$ and nutrient-enriched conditions. Other than this there is no study available from the Indian shelf (eastern Arabian Sea) or other parts of the Arabian Sea. This is important to note that with the reversal of monsoon (winter) in the southwest coast of India warm oligotrophic water with smaller phytoplankton dominance prevails (Viajayan et al. 2021; Albin et al. 2022) and may respond differently to the combined stress of Cu and OA. To fill this gap, the present study has been conducted during the winter monsoon to understand the collective impacts of Cu addition under a simulated OA scenario on the growth and community composition of the natural phytoplankton assemblages from the coastal as well as offshore waters of the Arabian Sea.

2. Materials and Methods

2.1. Sampling and experimental setup

Two microcosm incubation experiments were carried out onboard (*RV. Sindhu Sadhana*) during the winter monsoon (December 2019). The surface seawaters were collected (approximately 2.5 m considering the height of the CTD) with the help of Niskin samplers (24 No., each 10 L) fixed on a CTD-rosette (Sea-Bird, USA) from the eastern Arabian Sea (southwest shelf of India; 13.2°N and 73.69°E) for the first experiment (Exp-I) and central Arabian Sea (15°N and 64°E) for the second experiment (Exp-II) (Fig. 1). All bottles (polycarbonate Nalgene, USA) used for these experiments were pre-washed with 10% HCl followed by repeated MQ water. The collected water samples were directly transferred from the Niskin bottles into 12 Nalgene bottles (8 L) with the help of acid-cleaned Tygon tubes fitted with a 200 μm mesh (to avoid large copepods). Additional 2 bottles of equal volume were also filled to measure all the initial parameters (dissolved inorganic nutrients, carbon chemistry, phytoplankton biomass, cell density and enumeration, pigments). For each experiment, 12 bottles were filled, out of which 6 bottles were dedicated as the ambient CO_2 treatments (A- CO_2) and the rest 6 for high CO_2 (H- CO_2). $p\text{CO}_2$ manipulation was done by bubbling CO_2 (food-grade) gas from a cylinder and the pH drop was monitored to 7.8 using a precalibrated pH meter (Systronics, Kolkata) with standard buffers (Merck Chemicals). From the additional 2 bottles, the samples for measuring initial dissolved inorganic carbon (DIC) and total alkalinity (TA) were collected immediately in glass bottles with stoppers (100 mL for DIC and 250 mL for TA) and preserved with a few drops of HgCl_2 solution (1%) and closed tightly. For all DIC and TA samples, a parafilm strip was used to restrict the movement of the stoppers and kept inside a cardboard box at

room temperature until analysis. The DIC and TA samples for H-CO₂ treatments were collected soon after the manipulation of the CO₂ level was done.

Cu was added from a CuSO₄ (10 mM) stock solution to make the final concentration of 1 nM to both A-CO₂ and H-CO₂ treatments in triplicate (Fig. 1). After CO₂ manipulation and the addition of trace metal stock, the bottles were closed tightly and mixed gently. Then they were placed inside a water bath on the deck covered with a black nylon mesh to mimic the sunlight reaching 2.5 m depths. The water inside the bath was exchanged with the help of a continuous seawater flowing system on the deck to maintain the average water temperature close to the ambient water recorded from the CTD. The light intensity was measured every hour outside as well as inside the nylon mesh with the help of a lux meter (Metravi) and the values were converted to $\mu\text{mol Einstein m}^{-2} \text{ s}^{-1}$ with the coefficient provided by Thimijan and Heins (1983). A detail about the light intensity manipulation can be found in Shaik et al. (2017). The light intensities for the coastal and offshore experiments are given in supplementary Fig. 1a and 1b, respectively. The bottles were gently mixed every day at a particular time (10 am) to avoid biomass settlement and their positions inside the bath were exchanged to assure uniform light availability. This was noted in our previous studies that 72–96 hrs (3–4 days) was the average time for the tropical phytoplankton community to reach the exponential growth phase (Shaik et al. 2017; Sharma et al. 2020 and references therein). Accordingly, the bottles were incubated for 72 hours and were taken for further subsampling. Please note that this was a closed batch culture experiment and *p*CO₂ was manipulated only at the beginning of the experiment.

2.2. Analytical methods

2.2.1 Dissolved inorganic nutrients

Dissolved inorganic nutrients were analyzed immediately onboard following the standard spectrophotometric (UV-1800 UV-Vis Spectrophotometer, Shimadzu) methods. The concentrations of nitrate+nitrite and dissolved silicate (DSi) were estimated following the protocol of Grasshoff et al. (2009). Dissolved inorganic phosphate (DIP) was estimated following the method described by UNESCO (1994). All nutrient concentrations were calculated against the internal standard solutions as well as the certified reference material for ion chromatography (Multi anion Standard for nitrate and phosphate for Ion Chromatography P-code: 55698–100 mL; dissolved silicate 18895–100 mL, P-code 101955342, Sigma Aldrich, USA). For estimating biogenic silica (BSi) contents, an aliquot of 100 ml water sample was filtered onto a 0.2 μm (25 mm; GTTP, Millipore) filter using a plastic filtration unit. The filters were stored in plastic vials in the refrigerator. Before analysis, the filters

were oven-dried at 40 °C (8 hrs) and were analyzed for BSi contents following the method of Paasche (1973) against the standard Si solution (Sigma, USA).

2.2.2 Carbon chemistry parameters

DIC contents in seawater samples were analyzed (average error was < 2%) using a coulometer attached with an acidification module (UIC-CM 5015) against the certified reference material (Dickson batch 187). The TA of seawater was estimated by the potentiometric titration (against 0.1N HCl) method using international reference material (Dickson Batch 187) with the help of the Robotic titrosampler 855 from Metrohm (average error was < 5%). The final values of $p\text{CO}_2$ and pH were calculated in CO2SYS (pH in NBS scale; K1, K2 from Mehrbach et al. 1973 refit by Dickson and Millero 1987) (Pierrot et al. 2006) using DIC and TA along with DIP, DSi, salinity and temperature values.

2.2.3 Dissolved Cu levels

For analyzing the background dissolved Cu concentration, the experimental seawater samples were filtered (polycarbonate membrane Millipore, 0.45 μm , 47mm) immediately after the collection and acidified with ultra-pure HNO_3 (pH <2.0) and stored at -20°C for further analysis. Before analysis, these acidified samples were diluted up to 100 times with extra-pure water in the onshore laboratory. The dissolved Cu concentrations were estimated without matrix separation with High-Resolution ICP-MS (Model: *Nu instrument Attom ES*) equipped with a micro-nebulizer (Rodushkin and Ruth 1997) using ^{103}Rh solution as the internal standard. For checking the accuracy of the method, International Certified Reference Material SLEW-3 (NRC, Ottawa, Canada) was used and it exhibited a respectable agreement with the certified values (within 95% confidence; precision >5.0%).

2.2.4 Phytoplankton cell density and enumeration

Enumeration of phytoplankton was carried out by collecting 1-2 L samples in amber-colored PE bottles and fixed with Lugol's iodine solution (1%; w/v %) immediately after collection. In the laboratory, the sedimentation method was followed for 24 - 48 hours and the supernatant was discarded via a siphoning tube fitted with a 10 μm mesh to avoid the loss of phytoplankton cells to make the final volume of 20 - 30 mL. The cells were identified following the standard manuals (Tomas C. R 1997) and counted under an inverted microscope [Nikon (Ti2)] using an Utermohl counting chamber (Hydrobios Kiel, Germany) by taking a 3 mL subsample.

Phytoplankton species-specific growth rate (GR) was calculated based on the cell density found in the initial and final samples using the following formula

$$\text{Growth rate } (\mu \text{ d}^{-1}) = [\text{LN (final cell No.)} - \text{LN (initial cell No.)}] / \text{No. of day}$$

2.2.5 Phytoplankton pigment analysis using HPLC

For phytoplankton pigments analysis, 1 - 2 L of water samples were filtered using amber-colored filtration units onto GF/F filters (Whatman; 25 mm) under a low light condition. Immediately after filtration, the filters were stored in amber-colored Eppendorf tubes at -20°C for further analysis. Before analysis, the frozen filters were soaked in 5 mL ice-cold methanol (100%) (Merck chemicals, HPLC grade) overnight at -20°C for pigment extraction. The extracts were further filtered using a Teflon syringe (pore size 0.45 µm) for the removal of cellular debris. These filtered extracts were mixed manually with a buffer comprised of 28 mM aqueous tetra butyl ammonium acetate (TBAA; AR Grade, Fluka) at pH 6.5 and methanol in a 9:1 ratio. Phytoplankton pigments were quantified with the help of an HPLC (Shimadzu Prominence, LC2030) attached with a C8 Shimpack GIST column (pore size 3 µm) and photodiode array (PDA) detector, following the method described by Van Heukelem and Thomas (2001). Standard pigments from DHI (Netherlands) were used for the quantification and identification of the individual pigments. The peak area of the standard pigments was assessed to quantify the marker pigments.

2.2.6 Phytoplankton size class using phytopigments

The relative contribution of different size classes of phytoplankton was estimated by using the marker pigments [fucoxanthin (Fuco), 19'-hexanoyloxyfucoxanthin (19'HF), 19'-butanoyloxyfucoxanthin (19'BF), alloxanthin (Allo), Total Chlorophyll b (Chlb), peridinin (Perid), and zeaxanthin (Zea)]. The total sum of diagnostic pigments (DP_w) was calculated using the following formula (Uitz et al. 2006)

$$\Sigma(\text{DP})_w = (0.86)\text{Zea} + (1.01)\text{TChlb} + (0.60)\text{Allo} + (1.27)19'\text{HF} + (0.35)19'\text{BF} + (1.41)\text{Fuco} + (1.41)\text{Perid}$$

The concentrations of Chla associated with microphytoplankton, nanophytoplankton, and picophytoplankton were estimated following the equations based on the total content of DP (Vidussi et al. 2001).

$$\text{Micro (\%)} = [\{1.41 (\text{Fuco}) + 1.41 (\text{Perid})\} / \text{DP}_w] / 100$$

$$\text{Nano (\%)} = [\{1.27 (19'\text{HF}) + 0.35 (19'\text{BF}) + 0.60 (\text{Allo})\} / \text{DP}_w] / 100$$

$$\text{Pico (\%)} = [\{1.01 (\text{TChlb}) + 0.86 (\text{Zea})\} / \text{DP}_w] / 100$$

2.2.6 Statistical analysis

Statistical analysis was done using one-way and two-way analysis of variance (ANOVA) with replication (at 95% confidence level, probability (p) level 0.05) in MS excel 2016 to calculate the level of significance between the different treatments.

3. Results

3.1 Physicochemical variability

The ambient $p\text{CO}_2$ levels were 431 ± 18 μatm (Exp-I) and 456 ± 3.6 μatm (Exp-II) (Table 1). After manipulation, the H- CO_2 levels were 1238 ± 57 μatm (Exp-I) and 1100 ± 47.5 μatm (Exp-II). The background concentration of dissolved Cu in the offshore water was 1.82 ± 0.4 nM and in the coastal water, it was 2.4 ± 0.16 nM (Table 1). The initial nutrient concentrations were quite low during both experiments (Table 2). The concentrations of nitrate+nitrite and DIP were 0.22 ± 0.02 and 0.1 ± 0.005 $\mu\text{mol kg}^{-1}$, respectively in the shelf water. In the offshore water, nutrient concentrations were relatively higher (nitrate+nitrite and DIP were 3.28 ± 0.03 and 0.3 ± 0 $\mu\text{mol kg}^{-1}$, respectively). However, the dissolved silicate (DSi) levels were < 2 $\mu\text{mol Kg}^{-1}$ in both shelf (1.55 ± 0.05 $\mu\text{mol kg}^{-1}$) as well as offshore (1.95 ± 0.07 $\mu\text{mol kg}^{-1}$) waters (Table 2). Interestingly, high sea surface temperature (SST, 29°C) was observed in the southwestern shelf water, whereas in the offshore water the SST was 26°C . In Exp-I, the final DIP and nitrate+nitrite levels did not show any considerable difference from their initial value. Whereas, in Exp-II, the final nutrient levels except DIP were decreased in most of the treatments suggesting consumption during the experimental period (Table 2).

3.2. Phytoplankton biomass and growth rate

In shelf water, the initial Chl a concentration (Fig. 2a) was 0.067 ± 0.01 $\mu\text{g L}^{-1}$ and a 1.5 times increase was noticed in the post-incubated samples. But no significant difference between the treatments was seen ($p > 0.05$); Cu addition did not impact the concentrations of Chl a at any CO_2 level ($p > 0.05$). The microphytoplankton cell density (Fig. 2b) ($11.16 \pm 1.02 \times 10^3$ cells L^{-1}) did not show any significant change either under A- CO_2 or H- CO_2 treatments. However, the addition of Cu under the A- CO_2 level led to a considerable reduction ($p < 0.05$) in cell density (Fig. 2b); conversely, a 28% higher cell density ($p < 0.05$) under the H- CO_2 +Cu level was noticed relative to H- CO_2 control.

In offshore water, Chl a concentration (0.2 ± 0.02 $\mu\text{g L}^{-1}$) (Fig. 2c) increased significantly ($p < 0.05$) in the post-incubated samples, however, CO_2 or Cu induced changes were not significant ($p > 0.05$). The cell density increased in the post-incubated samples compared to the initial values. Elevated CO_2

supply resulted in 1.8-times ($p < 0.05$) enhancement in the cell density compared to A-CO₂. In A-CO₂+Cu treatment a $\approx 30\%$ reduction of cell density ($7.2 \pm 0.2 \times 10^4$ cells L⁻¹, $p < 0.05$) from the A-CO₂ control was recorded (Fig. 2d). However, under H-CO₂ treatments, Cu addition did not induce any noticeable change in cell density. BSi concentration (Fig. 2e) increased by 1.6 and 2.3 times ($p < 0.05$) compared to its initial value (0.5 ± 0.07 $\mu\text{mol L}^{-1}$) under A-CO₂ (0.9 ± 0.1 $\mu\text{mol L}^{-1}$) and H-CO₂ treatments (1.3 ± 0.2 $\mu\text{mol L}^{-1}$), respectively. A reduction of 30% in BSi concentration (Fig. 2e) was noted in the A-CO₂+Cu, but no such trend was noticed under the H-CO₂+Cu treatment.

3.3. Phytoplankton community and species-specific growth rates

In Exp-I, HPLC analysis detected several phytopigments in the experimental samples (supplementary Table 1). Pigment-based phytoplankton size class analysis showed that the initial sample was dominated by ($\approx 95\%$) Zea, a marker pigment for the group cyanobacteria representing picophytoplankton and with $< 5\%$ contribution of microphytoplankton (represented by Fuco) to the total Chl *a* (Fig. 3a). In the post incubated samples, an enhanced abundance of microphytoplankton (8 times) was seen, whereas picophytoplankton relative contribution decreased by 1.68 times. Nanophytoplankton, (most likely prymnesiophytes represented by 19'HF and 19'BF) contributed $< 1\%$ initially and was doubled in the post-incubated samples (Fig. 3a). It should be noted that using this method may also over or underestimate the contribution of diatoms to the microphytoplankton category as some smaller diatoms falling with the nanophytoplankton class may also contribute to Fuco contents.

The microphytoplankton community was mostly comprised of small dinoflagellates and diatoms (Table 3). Among the diatoms (Fig. 3b, 3c), the initial community was dominated by the pennate diatoms like *Nitzschia* sp. (1800 ± 471 cells L⁻¹; 17%), *Navicula* sp. (547 ± 37 cells L⁻¹; 5%), and *Cylindrotheca closterium* (87 ± 9 cells L⁻¹; 0.82%) and remained dominant after the incubation. The centric diatoms (mostly *Guinardia* sp. and a few *Rhizosolenia* sp.) showed a significant increase from 9.4% (initial) to 31.6% (A-CO₂) and 16% (H-CO₂). Interestingly, pennate diatom abundance enhanced to 98% (A-CO₂) and 95% (H-CO₂) in response to Cu addition, but centric diatoms decreased (Fig. 3b).

Enhanced CO₂ supply resulted in a 10 times higher GR (Fig. 3d) ($p < 0.05$) for *Nitzschia* sp. compared to the A-CO₂ control. Cu addition under the A-CO₂ level did not show any change in GR, however, under H-CO₂+Cu treatment GR increased by 1.88 times ($p < 0.05$). *Cylindrotheca closterium* was less abundant ($< 1\%$) initially, and increased 3-5 times ($p < 0.05$) under A-CO₂ and H-CO₂ levels, without any CO₂ enrichment effect. Cu addition under the A-CO₂ level resulted in ≈ 10

times decreased GR, but under H-CO₂+Cu, the GR remained unchanged. *Navicula* sp., in general, showed reduced cell density in all treatments without any significant variability (Fig. 3d). The most abundant centric diatom, *Guinardia* sp. was initially a minor contributor and exhibited net positive GRs, however, the high CO₂ supply resulted in 1.5 times lower GR compared to the A-CO₂ level ($p<0.05$). After the addition of Cu in the A-CO₂ and H-CO₂ levels, a 26 and 2.6 times decline ($p<0.05$) in the cell abundance was seen. The corresponding GR was negative under the A-CO₂+ Cu and it was positive at the H-CO₂+ Cu level, but the magnitude of growth inhibition was less than the former.

Among dinoflagellates (Fig. 3c), *Alexandrium* sp. (1020 ± 348 cells L⁻¹; 9.6%), *Gymnodinium* sp. (966 ± 160 cells L⁻¹; 9.16%), and *Gyrodinium* sp. (280 ± 94 cells L⁻¹; 2.64%) contributed almost 21.5% to the community. A small unidentified dinoflagellate was dominant (35%) initially and became undetectable in the post-incubated samples. The cell density of *Alexandrium* sp. reduced in the post-incubated samples with net negative GRs in all treatments. Cu addition led to a 78% (A-CO₂) and 32% (H-CO₂) decline in the cell density with a corresponding decline in GR (Fig. 3d) compared to the controls. The reduction in GR was the maximum in A-CO₂+Cu treatment (Fig. 3d). The cell density of the second abundant dinoflagellate *Gymnodinium* sp. was reduced to half in the post incubated treatments ($p<0.05$) with net negative GR. Cu addition in A-CO₂ level led to a 56% reduced cell density; whereas, under the H-CO₂+Cu treatment, the magnitude of decrease in GR was less.

In consistence with HPLC pigment analysis (supplementary table 1) showing the presence of 19'HF, *Phaeocystis* (Fig. 3c) was observed (953 ± 198 cells L⁻¹; 9.02%) under the microscope. The cell density was enhanced ($p<0.05$) under the A-CO₂ level (GR 0.41 ± 0.04 μ d⁻¹) (Fig. 3d) but remained unaffected at the H-CO₂ level ($p>0.05$). Under A-CO₂+Cu the GR decreased to 0.11 ± 0.07 μ d⁻¹ ($p<0.05$), however, no change was noted in H-CO₂+Cu treatment ($p>0.05$).

In Exp-II (offshore), the initial community was dominated by microphytoplankton (\approx 51%) containing Fuco (marker pigment for diatoms) followed by picophytoplankton (\approx 27%) and nanophytoplankton (\approx 10%) (Fig. 4a). No change ($p>0.05$) in the pigment-based community structure was noticed within the treatments. Pennate diatoms (91%) were the dominant followed by centric (9%) (Fig. 4b). With increasing CO₂ supply, 5% enhancement in pennate diatoms was noticed whereas the relative percentage of centric diatom was reduced to half ($p<0.05$). However, Cu addition did not cause any significant change in pennate and centric diatom abundance (Fig. 4b).

The initial phytoplankton community (Table 4; Fig. 4c) was dominated by pennate diatoms like *Pseudo-nitzschia* sp. (3586 ± 170 cells L^{-1} ; 50.39%), *Cylindrotheca closterium* (140 ± 9 cells L^{-1} ; 2.0%), *Navicula* sp. (126 ± 28 cells L^{-1} ; 1.8%), and *Nitzschia longissima* (46.6 ± 9.4 cells L^{-1} ; 0.66%). The average GR was higher in this experiment compared to Exp-I. Additional CO_2 supply reduced the GR of *Pseudo-nitzschia* sp. by 1.23 times ($p < 0.05$) compared to the A- CO_2 (Fig. 4d). The addition of Cu under A- CO_2 resulted in 1.4 times ($p < 0.05$) decline in GR of this genus. Whereas under the H- CO_2 +Cu treatment, the GR (0.82 ± 0.14) remained comparable ($p > 0.05$) with the H- CO_2 control (0.71 ± 0.07). *Cylindrotheca closterium* showed a 1.15 times reduction in the GR in the H- CO_2 treatment (0.97 ± 0.07) compared to the A- CO_2 (1.11 ± 0.04). After the addition of Cu, the cell density of this species reduced ($p < 0.05$) under the A- CO_2 ; whereas GR increased by 1.3 times ($p < 0.05$) under the H- CO_2 +Cu treatment compared to the H- CO_2 control. The GR of *Navicula* sp. was reduced 4 times in the H- CO_2 levels (0.28 ± 0.06) compared to the A- CO_2 control. In response to Cu addition under A- CO_2 , the GR was reduced by 1.5 times ($p < 0.05$) compared to the A- CO_2 control (1.1 ± 0.04). Interestingly, the highest GR of this species was seen in H- CO_2 +Cu treated samples with 2.73 times ($p < 0.05$) increase in GR from the H- CO_2 control. *Nitzschia longissima* contributed quite less (<1%) to the total community, but showed overall positive GR in all treatments. The increasing CO_2 showed an insignificant impact ($p > 0.05$), on the GR, however, the addition of Cu under both A- CO_2 and H- CO_2 led to a >1.2 times decrease ($p < 0.05$) in GR compared to the controls. The centric diatoms, *Guinardia flaccida* showed comparable GR under A- CO_2 (1.16 ± 0.2) and H- CO_2 (0.9 ± 0.04) treatments ($p > 0.05$). Cu addition under the A- CO_2 did not show any major change, but under the H- CO_2 level, GR was increased to 1.44 ± 0.12 .

The dominating dinoflagellate *Gymnodinium* sp. exhibited positive GR under the A- CO_2 and A- CO_2 +Cu without any noticeable difference. Conversely, negative GR was noticed in response to increasing CO_2 supply with and without Cu addition (Fig. 4d). Prymnesiophytic algae, *Phaeocystis* contributed (1907 ± 75 cells L^{-1}) almost 27% to the initial community. The high CO_2 addition increased the GR from 1.04 (A- CO_2) to 1.48 (H- CO_2) ($p < 0.05$). The addition of Cu under both CO_2 treatments showed unchanged GR ($p < 0.05$) compared to their controls.

4. Discussion

4.1. Physico-chemical variability and overall growth response

The Arabian Sea usually acts as a perennial source of atmospheric CO_2 and often exhibits higher pCO_2 levels than the atmospheric values (Sarma 2003; Valsala et al. 2021). The pCO_2 values in the A- CO_2 levels (≈ 450 μatm) are consistent with these observations. During the winter monsoon, the

northern Arabian Sea experiences convective mixing due to dry and cool northeast trade winds that intensify evaporation leading to surface cooling. This results in the upward transport of nutrients from the base of the mixed layer and upper thermocline (Prasanna Kumar and Prasad 1996) and increases primary productivity (Madhupratap et al. 1996). This mode of fertilization generally extends southward to at least 17° N (Naqvi et al. 2002) and not beyond this, and thus explains the occurrences of low nutrient concentrations in our experimental sites (shelf water; 13° N; offshore; 15° N). In shelf water (Exp-I), very low phytoplankton biomass, as well as the dominance of small phytoplankton, can be attributed to the low nutrient condition and also to some extent higher SST. Narvekar et al. (2017) also observed SST values as high as >28.5°C coupled with low phytoplankton biomass (0.1 -0.2 µg L⁻¹) in the south of 17° N during the winter months. Vijayan et al. (2021) reported the dominance of picoplanktonic prochlorophytes in warm nutrient-poor surface waters at 13° N. The smaller cells perform better under low nutrient availability, due to their high surface area to volume ratio (Marañón 2015). Besides, the increased temperature usually leads to enhanced respiration rates which make the cells smaller (Finkel et al. 2010). Whereas, in Exp-II (offshore community), the nutrient concentrations were slightly higher than the shelf water and could be the reason for the higher GR. But the DSi concentrations were <2 µM which can potentially hinder large diatom cell division and growth (Krause et al. 2019). In that case, either small-sized diatoms (with less DSi demand for growth) or other non-diatom smaller phytoplankton may dominate. The dominance of smaller pennate diatoms such as *Nitzschia* (coastal) and *Cylindrotheca closterium* (offshore) as well as the decline of large centric diatoms (*Rhizosolenia* sp., *Guinardia* sp.) in the H-CO₂ treatments, could be attributed to DSi limitations. This is important to mention that the DSi levels in the post-incubated samples were not exhausted indicating that these species might have the capability to grow and silicify under such low DSi levels. Moreover, the dead diatom frustules may also release some DSi (Kamatani and Riley, 1979) over the experimental period within the microcosms and could mask the actual consumption. Likewise, no noticeable difference between the initial and final DIP levels in both experiments also suggested that some amount of remineralized DIP might have been released. Importantly, phytoplankton may also consume organic phosphate as well as nitrogen under dissolved inorganic nutrient depletion. It has been noticed that the phytoplankton may considerably rely on organic nitrogen in the Arabian Sea (Shetye et al. 2019) and this also explains the insignificant nitrate+nitrite uptake in Exp-I.

Furthermore, in the shelf water experiment, the cell density did not show any significant change in the post-incubated samples, but *Chla* increased. This could be due to the increasing contribution of smaller phytoplankton which was not detectable under light microscopy. This fact is supported by

the HPLC-based pigment analysis which also revealed the dominance of picoplanktonic cyanobacteria (*Zea*) as well as nanoplanktonic prymnesiophytes which were enhanced in the post-incubated samples. The observation by Vijayan et al. (2021) also supported this view. The pigments 19'HF and 19'BF were most likely due to the presence of prymnesiophytes in our samples. The members of this group, mostly coccolithophores or *Phaeocystis*, were also documented earlier from the study region (Madhupratap et al. 2000; Balch et al. 2018).

4.2. Impacts of increasing CO₂

Biomass indicators such as *Chla* showed significant enhancement in response to elevated CO₂ supply despite oligotrophic conditions. Enhanced photosynthetic rate under a high CO₂ scenario could be attributed to increased *Chla* concentration. A marine diatom (*Thalassiosira pseudonana*; CCMP 1335) showed a 25% higher photosynthetic rate under the elevated CO₂ supply (Yang and Gao 2012). Liu et al (2016) reported the upregulation of certain enzymes that are required for *Chla* synthesis under increased CO₂ supply. Our previous studies showed the enhancement in the photosynthetic rate and *Chla* contents with increasing CO₂ levels in diatom-dominated phytoplankton communities from the Indian coastal waters (Biswas et al. 2011, 2017). However, in our previous study (Sharma et al. 2020) the simulated diatom community did not show any CO₂-induced increase in *Chla* contents.

The *p*CO₂ levels in the surface waters of the Arabian Sea can be high (>500 µatm) in the upwelling impacted regions during the southwest monsoon and showed a wide range of fluctuations (Körtzinger et al. 1997). Hence, the phytoplankton can be acclimatized to some extent to such *p*CO₂ variability; however, the level of acclimatization can be group/genus/species/strain-specific (Wolf et al. 2018). *Nitzschia* sp. and *Phaeocystis* sp. in Exp-I and only *Phaeocystis* sp. in Exp-II exhibited a positive growth response to elevated CO₂ supply. Enhanced CO₂ can exert diverse impacts on phytoplankton photosynthetic performance and GR which in turn are related to their carbon dioxide concentration mechanisms (CCMs) (Giordano et al. 2005). The phytoplankton species that depend on the diffusive uptake of CO₂ can show stimulatory response under H-CO₂ compared to those species which are using HCO₃⁻ or CO₂ via CCMs (Beardall et al. 2009). The growth enhancement due to increasing CO₂ supply may depend on the difference between diffusion of CO₂ within the cell and efficient carboxylation. Several factors determine DIC accumulation in the vicinity of the carboxylation site and phytoplankton cell size is one of them (Malerba et al. 2020). Due to the high surface area to volume ratio, the small cells could acquire a sufficient amount of DIC compared to their larger siblings which are having less surface to volume ratio (Raven 1987; Finkel et al. 2010). Thus small cells would be expected to show a higher GR under elevated CO₂ conditions (Sun et al.

2011; Tatters et al. 2012) as seen in the case of *Nitzschia* sp. and *Phaeocystis* sp. in our experiments. The predominance of *Nitzschia* under the H-CO₂ treatments was also documented in our previous study (Sharma et al. 2020, 2021). Likewise, a high cell number of *Phaeocystis* (<10⁶ cells mL⁻¹) was also reported from the central Arabian Sea close to our sampling stations by Moffett et al. (2015) during the southwest monsoon. In our recent study (Sharma et al. 2021), 19'HF containing prymnesiophytic algae responded positively under H-CO₂ supply (800 µatm). *Phaeocystis globosa* exhibited lower sensitivity to very high CO₂ levels (>1500µatm) in the experimental study (Rost et al. 2003), and this was probably related to DSi limitation which restricted diatom growth. It was noted in a subtropical phytoplankton community that the high CO₂ level promoted the growth of the prymnesiophytic algae *Phaeocystis globosa* (Taucher et al. 2018).

Bach and Taucher (2019) reviewed 54 available studies on the impacts of increasing CO₂ levels on marine diatoms and pointed out only 19% of them showed negative responses to the elevated CO₂ levels. In our study, among other major contributing genera, high CO₂-induced negative GR was seen in 3 diatoms (*Navicula* sp., *Pseudo-nitzschia* sp., *Cylindrotheca closterium*) in offshore water and one (*Guinardia* sp.) in shelf water. This is important to note that *Guinardia* and *Pseudo-nitzschia* sp showed a positive growth response in a previous study (Sharma et al. 2020) conducted during the SW monsoon from the southeastern Arabian Sea. However, also showed a negative GR in another study during the winter monsoon from a similar location (Sharma et al. 2021). Such a contradictory response of the same genus to the elevated CO₂ levels can be related to their species-specific or strain-specific carbon metabolism pathways (Wolf et al. 2018). A negative growth response suggested inhibited cell division due to the increasing CO₂ levels or decreasing pH. This is possible that these diatoms were not able to benefit from energy savings related to elevated CO₂ supply. On the other hand, a low pH may induce higher respiration rates (Wu et al. 2010) and thus may demand higher energy and could lead to slow or negative GR. The increasing pCO₂ (carbonation) and associated decreasing pH may separately have a complex impact on diatom photosynthetic and respiration rates (Goldman et al. 2017). A recent study where pCO₂ and pH were independently varied found no noticeable effects of either pCO₂ or pH change on growth, photosynthesis, or respiration in the marine diatom *Thalassiosira weissflogii* (Goldman et al. 2017). Wu et al. (2017) showed that changes in CO₂, and not pH, dominated the photochemical responses of the model *Phaeodactylum tricornerutum* to OA. Based on this physiological plasticity of the individual genus, species, or strain at the elevated CO₂ levels, the winners and losers are usually determined, and hence is important to understand for predicting the community shift in the future ocean.

A total of 3 diatoms (*Cylindrotheca closterium* in shelf water; *Guinardia flaccida* and *Nitzschia longissima* in offshore water) showed neutral GR in response to enhanced CO₂ supply. A neutral response can be expected when these diatoms can adjust their energy and resource requirements under such variable CO₂ levels ($\approx 400 - 1200 \mu\text{atm}$). In the review by Bach and Taucher (2019), it was seen that out of 19 high CO₂ incubation experiments from the oceanic communities, 32% revealed no impact. Likewise, the study by Boelen et al. (2011) found that variable CO₂ levels did not show any impact on the photosynthetic performance as well as GR of a marine diatom *Chaetoceros brevis*. The authors postulated that the expected energy savings by the downregulation of CCMs can be negligible to be used for growth enhancement which can be present for the other species with positive GR (Hopkinson et al. 2011). This could be related to resource limitation (e.g. nutrients) which controls the amount of saved energy related to CCM operation (Boelen et al. 2011). No change in GR in response to elevated CO₂ was also noticed by Burkhard et al. (1999) in marine diatoms. Young et al. (2015) observed the downregulation of CCMs in response to a doubling of CO₂ supply from 400 μatm without any modification in GR in a diatom-dominated phytoplankton assemblage from the Antarctic.

In both experiments, the dinoflagellates (*Gymnodinium* sp. *Alexandrium* sp.) were the worst impacted at the elevated CO₂ levels and showed negative GR. A similar trend was also observed by Taucher et al. (2018) where dinoflagellates displayed a negative response to higher CO₂ under oligotrophic conditions. On the contrary, in some laboratory studies, dinoflagellates exhibited tolerance/positive growth at elevated CO₂ levels (Fu et al. 2008; Eberlein et al. 2014). Increased abundance of dinoflagellates like *Prorocentrum* and *Peridinium* was also documented under H-CO₂ levels in our earlier study (Sharma et al. under review). Hattenrath-Lehmann et al. (2015) noticed that certain species of *Alexandrium* exhibited a positive growth response and increased toxin production under the elevated CO₂ supply. This type of contradictory response could also be due to the community composition and competitive efficiency for nutrient uptake (Wolf et al. 2018). The mixotrophic dinoflagellate, namely *Gymnodinium* sp., and *Alexandrium* sp may decline due to the indirect effect of H-CO₂ via the food web (Taucher et al. 2018) imposed by the unavailability of the preferred prey. Particularly, the prymnesiophytic algae in the post-incubated samples may not be preferably grazed by the mixotrophic dinoflagellate.

4.3. Impacts of Cu addition and interaction with increasing CO₂

The community shift induced by the enrichment of Cu under the A-CO₂ suggested that most of the phytoplankton species are likely to be sensitive to Cu toxicity. Cu is one of the most important bioactive trace metals and plays a major role in cellular physiology (Sunda 2012), and makes the

strongest complexes with the ligands among other trace metals (Waldron et al. 2009). During Exp-I, higher SST (29°C) and oligotrophy might have synergistically hindered the growth. Several environmental factors such as OA and temperature can alter metal speciation in the marine environment and therefore, could change the bioavailability and toxicity of metals in marine biota (Millero et al. 2009). Increased temperature can result in reduced reproduction and high mortality in phytoplankton as it enhances the uptake and accumulation rate of trace metals (Wang and Wang 2008; Yung et al. 2017). Several studies showed enhanced toxicity of Cu with increasing temperature in diatoms and green algae (Morin et al. 2017; Silva et al. 2018).

An earlier study by Guo et al. (2012) showed that the role of Cu in marine phytoplankton physiology was more prominent for offshore strains compared to those in coastal waters. The authors noted that the cellular highest average Cu quotas showed the following trend: bacillariophyceae > cyanophyceae > prymnesiophyceae > dinophyceae. The observed decline in dinoflagellate abundance in response to elevated Cu concentration also supports this fact. This trend indicates that depending on the actual cellular Cu quota, the toxic impact may differ in the individual algal group. Higher resilience was seen in bacillariophyceae and prymnesiophyceae compared to dinophyceae. This is important to note that Cu addition may also induce toxicity to the grazers and phytoplankton biomass may show enhancement due to reduced grazing pressure related to Cu addition (Stoecker et al. 1986).

In our study, Cu addition at the A-CO₂ level did not impact the net Chl*a* concentrations, but the cell density decreased. Increased positively charged metal ions (M⁺) flow inside the cell may attack the active sites of nucleic acids and proteins and thus hinders cell division (Masmoudi et al. 2013). Nguyen-Deroche et al. (2009) also observed that in marine diatoms, Cu addition impacted photosynthetic performance without impacting the net Chl*a* content. Some studies reported a significant decline in the cell density and GR but enhancement in the cell size with elevated Cu concentration (Sunda and Huntsman 1986; Fisher et al. 1981), and this could be because of the uncoupling between the cell division and photosynthetic rate which results in the accumulation of photosynthetic product within the cell (Hall et al. 1989; Yang et al. 2019). In several experiments, Cu addition was shown to reduce the cell density in marine diatoms (Cid et al. 1995; Nguyen-Deroche et al. 2009). The addition of Cu in a model marine diatom was shown to impact DNA synthesis and cell cycle within 2 days of incubation (Wei et al. 2014) and explains the reason for restricted cell division. Moreover, in the case of diatoms, any interruption in silicification may directly hinder the cell division rates. The reduced BSi production in Exp-II in the A-CO₂+Cu treatment indicated that Cu addition inhibited the silicification process. Si and Cu ions compete for the same protein

transporter and therefore elevated Cu concentration may inhibit the silicate uptake and thus BSi production in marine diatoms (Rueter and Morel 1981). A similar observation was noticed in our previous studies (Biswas and Bandyopadhyay 2017).

The interesting observation from both the experiments was *Nitzschia* (in shelf water) along with *Guillardia flaccida* and *Cylindrotheca* (in offshore water) showed higher GR under HCO₂+Cu treatment suggesting that these phytoplankton taxa probably possess higher cellular Cu demand. An enhanced abundance of *Nitzschia* under HCO₂+Cu treatments was also documented in our previous study (Sharma et al. 2020) from the southeastern Arabian Sea. *Nitzschia* showed its high potential to cope with elevated Cu levels and could be the reason for forming bloom in the upwelling and polluted waters (Morin et al. 2012). In both experiments, *Phaeocystis* grew exponentially under Cu enriched samples, at elevated CO₂ levels which could be due to higher Cu demand for growth. Lombardi and Maldonado (2011) observed in a laboratory experiment that enhanced Cu supply did not show any impact on photosystem II function of *Phaeocystis*. The observations by Guo et al. (2012) and Lombardi and Maldonado (2011) collectively suggest that prymnesiophytes might be having higher Cu tolerance and more Cu requirement than other phytoplankton groups. Moffett et al. (2015) also observed a *Phaeocystis* bloom under DSi limitation during an onboard incubation experiment from the central Arabian Sea and added Cu was found to have a negligible impact on Chla values.

The phytoplankton cell surface is usually surrounded by several functional groups (carboxylic, thiol, amino, hydroxy, and hydroxy-carboxylic) (Gonzdez-Drivilal, M. 1995). Under enhanced free metal concentrations (either due to an increased supply of dissolved metal or lowering of pH) these functional groups scavenge the M⁺ outside the cell and the toxicity can be minimized to some extent owing to the limited numbers of such functional groups (Gonzdez-Drivilal M. 1995). When the proton (H⁺) concentrations increase, a consequent competition between the H⁺ and M⁺ occurs to attach with the functional groups, and H⁺ replaces the M⁺ resulting in increased M⁺ availability (Millero et al. 2009). These metal ions can be transported inside the cell (cytosol) and could attach nonspecifically with the coordination sites (active site) of biomolecules like enzymes and may alter the normal metabolic functions (Sunda 1989). Phytoplankton cells possess several mechanisms to reduce such metal toxicity by producing metal-binding compounds using specific enzymes like superoxide dismutase and by synthesizing other proteins like glutathione (GSH) and phytochelatins (PCs) to chelate the free metal ions (Kawakami et al. 2006a, b) followed by exclusion of the chelated metals from the cell (Waldron et al. 2009; Masmoudi et al. 2013).

Some studies (Dong et al. 2020a, 2020b) noticed that the model marine diatoms (*Skeletonema costatum* and *Phaeodactylum tricornutum*) were able to alleviate metal (e.g. Cd) toxicity when grown under high $p\text{CO}_2$ levels (1500 μatm). A similar study was conducted by Xu et al. (2021) and it was noticed that three marine diatoms (*Phaeodactylum tricornutum*, *Thalassiosira pseudonana*, and *Chaetoceros mulleri*) were able to tolerate metal stress (arsenic) under increasing $p\text{CO}_2$ levels (1000 and 2000 μatm) over the short term as well as long term exposure. To understand the mechanism for metal stress alleviation under OA, the cellular energy allocation for multiple processes needs to be discussed. Carbonic anhydrase (CA) plays a central role in diatoms CCMs by converting the bicarbonate ions to CO_2 and was shown to be inhibited by Cu toxicity in the marine diatoms (Nguyen-Deroche et al. 2009). Consequently, under A- CO_2 +Cu, CCM-mediated DIC export inside the cell can be severely hampered. Conversely, when CO_2 supply is enhanced, CA-dependent DIC acquisition can be downregulated due to higher CO_2 diffusive influx. And therefore under H- CO_2 +Cu treatment, Inhibited CA activity due to Cu toxicity may not be crucial for carbon transport keeping the photosynthetic rate unaltered. Phytoplankton cells may benefit from the increasing CO_2 supply and enhance photosynthetic products which may help in alleviating metal stress under the OA scenario. Likewise, the study by Wu et al. (2014) on five diatom species revealed that increased CO_2 supply resulted in the production of higher photosynthetic reductants which was responsible for faster growth. As mentioned earlier that to reduce metal toxicity several specific enzymes enriched with thiol group and compounds like GSH and PCs synthesis are required which is expensive in terms of cellular resources and energy. Besides, Cu addition was found to enhance the respiration rates in marine diatoms suggesting higher energy requirements mostly to reduce metal toxicity (Nguyen-Deroche et al. 2009). Therefore, the energetic savings and increased production of photosynthates under OA may facilitate the synthesis of these detoxifying compounds.

High light and some metals like Cu, Cd, both stressors generate reactive oxygen species inside the cell and can be highly deleterious for photosystems (Rijstenbil et al. 1994; Manimaran et al. 2012). The alleviation of light stress under OA was also noticed in unicellular green algae (Garcia-Gomez et al. 2014) as well as in coastal diatoms (Biswas et al. 2014). Valenzuela et al. (2018) reported that the marine diatom *Thalassiosira pseudonana* showed higher resilience under OA as well as high light and low nitrogen, a condition that is likely to prevail in the future oceans. Under OA, low pH may induce higher respiration rates (Wu et al. 2010) and thus may demand higher energy. At the same time, the down-regulation of CCMs may provide some energetic savings (Giordano 2005; Hopkins 2011) and may increase photosynthates inside the cell (Shaik et al. 2017). Consequently, CO_2 -induced higher growth may demand more Cu for building the essential Cu-proteins like

plastocyanin, cytochrome oxidase, and multicopper oxidase involved in the photosynthetic light reaction, respiratory electron transport, and Fe acquisition, respectively (Kong and Price 2020). In that case, Cu removal for growth is likely to increase with a subsequent reduction of the toxic level inside the cell. Whereas, in the case of A-CO₂+Cu treatments, the dissolved Cu (>1 nM) level was probably enough for supporting growth and the additional Cu supply exerted a toxic impact. The projected oligotrophy induced by warming and increasing CO₂ levels in combination with Cu pollution may potentially alter the phytoplankton community both in the shelf as well as offshore waters of the Arabian Sea.

Conclusions

Multiple stressor studies are usually difficult to handle due to the complexity of the matrix of variables, yet are becoming increasingly important in the context of climate change and are scarce from the Indian Ocean region. We present here the second report on the combined stressor [trace metal (Cu) enrichment and ocean acidification] from the southwestern shelf of India and the first experimental study from the central Arabian Sea. In this study, which was conducted during the winter monsoon on the natural phytoplankton communities, we observed that increasing CO₂ levels exhibited a growth-stimulating impact in some phytoplankton, whereas, a few responded negatively. The addition of 1 nM Cu under the A-CO₂ level significantly inhibited cell density without impacting Chl_a concentrations. Interestingly, 1 nM Cu addition under the elevated CO₂ level did not show a change in phytoplankton cell numbers or biomass. Species like *Nitzschia* and *Phaeocystis* showed higher growth responses to both CO₂ as well as Cu enrichment, and this could be attributed to the higher cellular Cu demand of these species. Low DSi levels could also be one of the reasons for promoting non-diatom phytoplankton like *Phaeocystis*. Moreover, the addition of CO₂ seemed to reduce the toxic impacts of Cu in some phytoplankton species. Such response was not observed in the previous study (Sharma et al. 2020) which was conducted during the southwest monsoon-induced upwelling. In that study, a phytoplankton community dominated by diatoms was grown under nutrient-replete conditions onboard and the background dissolved Cu level was nearly 11 nM. Neither cell division nor the Chl_a contents were impacted in response to Cu (1 nM) addition in any CO₂ levels. Contrarily, during the present study at the time of the winter monsoon, the southwestern shelf water becomes warm and oligotrophic with very less diatom abundance; and the dissolved Cu level was 4.6 times lower compared to the southwest monsoon. All these differences in the physicochemical parameters, particularly nutrient availability as well as the phytoplankton community composition were probably the reason for a different response, although some were comparable. Likewise, species like *Nitzschia* and *Pseudo-nitzschia* revealed positive growth

responses in the previous study confirming their high Cu and CO₂ tolerance and could potentially bloom in the future in this region. Such a community shift may have a considerable impact on grazing, the food chain, and carbon transfer in this area. This should be mentioned that the Arabian Sea is a perennial source of atmospheric CO₂ and some phytoplankton are likely to show resilient behavior, but their response can be different when considering other stress factors like increasing temperature and stratification leading to oligotrophy and aerosol dust flux. Whether these factors will impact the natural phytoplankton community in an antagonistic or synergistic way is still not understood and needs to be addressed in future studies. And while planning such experiments high spatial and seasonal variability in primary production and phytoplankton community composition in the Arabian Sea should be considered. Nonetheless, this is important to improve our mechanistic understanding to justify such species-specific responses to multiple stressors and that may help to predict the future phytoplankton community shift in these tropical waters. It should be noted that the experiments conducted on a natural community provide the basic information on the species-specific response and the competitive efficiency to the simulated stressed factors. However, the species showing resilient behavior in such natural assemblages can be used to develop monoculture and further experiments are recommended to monitor the enzymatic expression and reprogramming of cellular mechanisms related to the specific stress using molecular tools.

Acknowledgment: The first author is grateful to the DST-Inspire fellowship program for financial support and also to Bharathidasan University staff for their technical help concerning her Ph.D. registration. We acknowledge the generous efforts made by the crew members, the captain of the SSD 68 cruise, the ship cell, and other colleagues of CSIR-NIO. This work was carried out under the project MLP-1802. The active support from the director, CSIR-NIO is gratefully acknowledged. For pigment and dissolved trace metals analyses, the central analytical facility was used at the CSIR-NIO and we are thankful to Ms. Teja Naik and Mr. Robin John for their technical help. NIO's contribution number is XXXX. We thank the anonymous reviewers for their thoughtful evaluation and comments to improve the manuscript.

Statements and Declarations

Funding: The basic funding for this study was provided by the Council of Scientific and Industrial Research (CSIR); the first author's fellowship is funded by the Department of Science and Technology (DST) Inspire Fellowship program. The second and the third authors were funded by University Grant Commission (UGC) India and CSIR; the fourth author is financially supported by the DST. NIO contribution number is XXXX (will be provided after the acceptance of the paper).

Conflict of Interest: The authors declare that the research was conducted in the absence of any commercial or financial relationships that could be construed as a potential conflict of interest.

Authors statement: Diksha Sharma and Haimanti Biswas contributed to the study conception and design. Material preparation, data collection, and analysis were performed by Diksha Sharma, Haimanti Biswas, Mintu Chowdhury, Saumya Silori, Medhavi Pandey, and Durbar Ray. The first draft of the manuscript was written by Diksha Sharma and all authors commented on previous versions of the manuscript. All authors read and approved the final manuscript.

Availability of data and materials: All data related to this study are presented in this manuscript.

Conflict of interest: The authors declare no competing interests.

Ethical Approval: Not Applicable

Consent to Participate: Not applicable

Consent to Publish: Not applicable

References

- Bach LT, Taucher J (2019) CO₂ effects on diatoms: a synthesis of more than a decade of ocean acidification experiments with natural communities. *Ocean Sci* 15(4):1159-1175. <https://doi.org/10.5194/os-15-1159-2019>
- Balch WM, Bowler BC, Drapeau DT, Lubelczyk LC, Lyczkowski E (2018) Vertical distributions of coccolithophores, PIC, POC, biogenic Silica, and chlorophyll a throughout the global ocean. *Global Biogeochem Cycles* 32(1):2-17. <https://doi.org/10.1002/2016GB005614>
- Beardall J, Stojkovic S, Larsen S (2009) Living in a high CO₂ world: impacts of global climate change on marine phytoplankton. *Plant Ecol Divers* 2(2):191-205. <https://doi.org/10.1080/17550870903271363>
- Biswas H, Alexander CROS, Yadav K, Ramana VV, Prasad VR, Acharyya T, Babu PR (2011) The response of a natural phytoplankton community from the Godavari River Estuary to increasing CO₂ concentration during the pre-monsoon period. *J Exp Mar Biol Ecol* 407(2):284-293. <https://doi.org/10.1016/j.jembe.2011.06.027>
- Biswas H, Bandyopadhyay D (2017) Physiological responses of coastal phytoplankton (Visakhapatnam, SW Bay of Bengal, India) to experimental copper addition. *Mar Environ Res* 131:19-31. <https://doi.org/10.1016/j.marenvres.2017.09.008>
- Biswas H, Shaik AUR, Bandyopadhyay D, Chowdhury N (2017) CO₂ induced growth response in a diatom dominated phytoplankton community from SW Bay of Bengal coastal water. *Estuar Coast Shelf Sci* 198:29-42. <https://doi.org/10.1016/j.ecss.2017.07.022>

- Biswas H, Shaik, AUR, Bandyopadhyay D (2014) Preliminary evidences of CCM operation and its down regulation in relation to increasing CO₂ levels in natural phytoplankton assemblages from the coastal waters of Bay of Bengal. In *EGU General Assembly Conference Abstracts*, 336. <https://ui.adsabs.harvard.edu/#abs/2014EGUGA..16..336B/abstract>
- Boelen P, Van De Poll WH, Van Der Strate HJ, Neven IA, Beardall J, Buma AG (2011) Neither elevated nor reduced CO₂ affects the photophysiological performance of the marine Antarctic diatom *Chaetoceros brevis*. *J Exp Mar Biol Ecol* 406(1-2):38-45. <https://doi.org/10.1016/j.jembe.2011.06.012>
- Cid A, Herrero C, Torres E, Abalde J (1995) Copper toxicity on the marine microalga *Phaeodactylum tricorutum*: effects on photosynthesis and related parameters. *Aquat Toxicol*, 31(2):165-174. [https://doi.org/10.1016/0166-445X\(94\)00071-W](https://doi.org/10.1016/0166-445X(94)00071-W)
- Coale KH, Bruland KW (1990) Spatial and temporal variability in copper complexation in the North Pacific. *Deep Sea Res Part I Oceanogr Res Pap* 37(2):317-336. [https://doi.org/10.1016/0198-0149\(90\)90130-N](https://doi.org/10.1016/0198-0149(90)90130-N)
- DeVries T, Holzer M, Primeau F (2017) Recent increase in oceanic carbon uptake driven by weaker upper-ocean overturning. *Nature* 542(7640):215-218. <https://doi.org/10.1038/nature21068>
- Doney SC, Fabry VJ, Feely RA, Kleypas JA (2009) Ocean acidification: the other CO₂ problem. *Ann Rev Mar Sci* 1:169-192. <https://doi.org/10.1146/annurev.marine.010908.163834>
- Dong F, Wang P, Qian W, Tang X, Zhu X, Wang Z, Wang J (2020) Mitigation effects of CO₂-driven ocean acidification on Cd toxicity to the marine diatom *Skeletonema costatum*. *Environ Pollut* 259:113850. <https://doi.org/10.1016/j.envpol.2019.113850>
- Dong F, Zhu X, Qian W, Wang P, Wang J (2020) Combined effects of CO₂-driven ocean acidification and Cd stress in the marine environment: Enhanced tolerance of *Phaeodactylum tricorutum* to Cd exposure. *Mar Pollut Bull* 150:110594. <https://doi.org/10.1016/j.marpolbul.2019.110594>
- Eberlein T, Van de Waal DB, Rost B (2014) Differential effects of ocean acidification on carbon acquisition in two bloom-forming dinoflagellate species. *Physiol Plant* 151(4):468-479. <https://doi.org/10.1111/ppl.12137>
- Eichler A, Tobler L, Eyrikh S, Malygina N, Papina T, Schwikowski M (2014) Ice-core based assessment of historical anthropogenic heavy metal (Cd, Cu, Sb, Zn) emissions in the Soviet Union. *Environ Sci Technol* 48(5):2635-2642. <https://doi.org/10.1021/es404861n>
- Finkel ZV, Beardall J, Flynn KJ, Quigg A, Rees TAV, Raven JA (2010) Phytoplankton in a changing world: cell size and elemental stoichiometry. *J Plankton Res* 32(1):119-137. <https://doi.org/10.1093/plankt/fbp098>
- Fisher NS, Jones GJ, Nelson DM (1981) Effects of copper and zinc on growth, morphology, and metabolism of *Asterionella japonica* (Cleve) 1. *J Exp Mar Biol Ecol* 51(1):37-56. [https://doi.org/10.1016/0022-0981\(81\)90153-2](https://doi.org/10.1016/0022-0981(81)90153-2)
- Fu FX, Zhang Y, Warner ME, Feng Y, Sun J, Hutchins DA (2008) A comparison of future increased CO₂ and temperature effects on sympatric *Heterosigma akashiwo* and *Prorocentrum minimum*. *Harmful algae* 7(1):76-90. <https://doi.org/10.1016/j.hal.2007.05.006>

- Garcia-Gomez C, Gordillo FJ, Palma A, Lorenzo MR, Segovia M (2014) Elevated CO₂ alleviates high PAR and UV stress in the unicellular chlorophyte *Dunaliella tertiolecta*. *Photochem Photobiol Sci* 13(9):1347-1358. <https://doi.org/10.1039/C4PP00044G>
- Giordano M, Beardall J, Raven JA (2005) CO₂ concentrating mechanisms in algae: mechanisms, environmental modulation, and evolution. *Annu Rev Plant Biol* 56:99-131. <https://doi.org/10.1146/annurev.arplant.56.032604.144052>
- Goldman JA, Bender ML, Morel FM (2017) The effects of pH and pCO₂ on photosynthesis and respiration in the diatom *Thalassiosira weissflogii*. *Photosynth Res* 132(1):83-93. <https://doi.org/10.1007/s11120-016-0330-2>
- González-Dávila M (1995) The role of phytoplankton cells on the control of heavy metal concentration in seawater. *Mar Chem* 48(3-4):215-236. [https://doi.org/10.1016/0304-4203\(94\)00045-F](https://doi.org/10.1016/0304-4203(94)00045-F)
- Grasshoff K, Kremling K, Ehrhardt M (Eds.) (2009) *Methods of seawater analysis*. John Wiley & Sons.
- Guo J, Lapi S, Ruth TJ, Maldonado MT (2012) The effects of iron and copper availability on the copper stoichiometry of marine phytoplankton. *J Phycol* 48(2):312-325. <https://doi.org/10.1111/j.1529-8817.2012.01133.x>
- Hall J, Healey FP, Robinson GGC (1989) The interaction of chronic copper toxicity with nutrient limitation in two chlorophytes in batch culture. *Aquat Toxicol* 14(1):1-13. [https://doi.org/10.1016/0166-445X\(89\)90051-9](https://doi.org/10.1016/0166-445X(89)90051-9)
- Hattenrath-Lehmann TK, Smith JL, Wallace RB, Merlo LR, Koch F, Mittelsdorf H, Goleski JA, Anderson DM, Gobler CJ (2015) The effects of elevated CO₂ on the growth and toxicity of field populations and cultures of the saxitoxin-producing dinoflagellate, *Alexandrium fundyense*. *Limnol Oceanogr* 60(1):198-214. <https://doi.org/10.1002/lno.10012>
- Hopkinson BM, Dupont CL, Allen AE, Morel FM (2011) Efficiency of the CO₂-concentrating mechanism of diatoms. *PNAS*, 108(10):3830-3837. <https://doi.org/10.1073/pnas.1018062108>
- IPCC 2013. In: Stocker TF, Qin D, Plattner GK, Tignor M, Allen SK, Boschung J, Nauels A, Xia Y, Bex V, Midgley PM (Eds) *Climate Change 2013: the Physical Science Basis*. Contribution of Working Group I to the Fifth Assessment Report of the Intergovernmental Panel on Climate Change. Cambridge University Press, Cambridge, United Kingdom and New York, NY, USA, 1535.
- Irving HMNH, Williams R (1953). The stability of transition-metal complexes. *J Chem Soc (Resumed)* 3192-3210.
- Jordi A, Basterretxea G, Tovar-Sánchez, A., Alastuey, A., and Querol, X. (2012). Copper aerosols inhibit phytoplankton growth in the Mediterranean Sea. *PNAS* 109(52):21246-21249. <https://doi.org/10.1073/pnas.1207567110>
- Kamatani A, Riley JP (1979) Rate of dissolution of diatom silica walls in seawater. *Mar Biol* 55(1): 29-35. <https://doi.org/10.1007/BF00391714>

- Kawakami SK, Gledhill M, Achterberg EP (2006a) Determination of phytochelatins and glutathione in phytoplankton from natural waters using HPLC with fluorescence detection. *Trends Analyt Chem* 25(2):133-142. <https://doi.org/10.1016/j.trac.2005.06.005>
- Kawakami SK, Gledhill M, Achterberg EP (2006b) Production of phytochelatins and glutathione by marine phytoplankton in response to metal stress 1. *J Phycol* 42(5):975-989. <https://doi.org/10.1111/j.1529-8817.2006.00265.x>
- Kong L, Price NM (2020) Identification of copper-regulated proteins in an oceanic diatom, *Thalassiosira oceanica* 1005. *Metallomics* 12(7):1106-1117. <https://doi.org/10.1039/d0mt00033g>
- Körtzinger A, Duinker JC, Mintrop L (1997) Strong CO₂ emissions from the Arabian Sea during south-west monsoon. *Geophys Res Lett* 24(14):1763-1766. <https://doi.org/10.1029/97GL01775>
- Krause JW, Schulz IK, Rowe KA, Dobbins W, Winding MH, Sejr MK, Duarte CM Agustí S (2019) Silicic acid limitation drives bloom termination and potential carbon sequestration in an Arctic bloom. *Sci Rep* 9(1):1-11. <https://doi.org/10.1038/s41598-019-44587-4>
- Prasanna Kumar, Prasad TG (1996) Winter cooling in the northern Arabian Sea. *Curr Sci* 834-841.
- Liao X, Zhan H, Du Y (2016) Potential new production in two upwelling regions of the western Arabian Sea: Estimation and comparison. *J Geophys Res Oceans* 121(7):4487-4502. <https://doi.org/10.1002/2016JC011707>
- Liu F, Li S, Zheng F, Huang X (2016) Risk assessment of excessive CO₂ emission on diatom heavy metal consumption. *Sci Total Environ* 566:1349-1354. <https://doi.org/10.1016/j.scitotenv.2016.05.196>
- Lombardi AT, Maldonado MT (2011) The effects of copper on the photosynthetic response of *Phaeocystis cordata*. *Photosynth Res* 108(1):77-87. <https://doi.org/10.1007/s11120-011-9655-z>
- Lopez JS, Lee L, Mackey KR (2019) The toxicity of copper to *Crocospaera watsonii* and other marine phytoplankton: a systematic review. *Front Mar Sci* 5:511. <https://doi.org/10.3389/fmars.2018.00511>
- Madhupratap M, Kumar SP, Bhattathiri PMA, Kumar MD, Raghukumar S, Nair KKC, Ramaiah N (1996) Mechanism of the biological response to winter cooling in the northeastern Arabian Sea. *Nature*, 384(6609):549-552.
- Madhupratap M, Sawant S, Gauns M (2000) A first report on a bloom of the marine prymnesiophycean, *Phaeocystis globosa* from the Arabian Sea. *Oceanol Acta* 23(1):83-90. [https://doi.org/10.1016/S0399-1784\(00\)00109-2](https://doi.org/10.1016/S0399-1784(00)00109-2)
- Mahowald NM, Hamilton DS, Mackey KR, Moore JK, Baker AR, Scanza RA, Zhang Y (2018) Aerosol trace metal leaching and impacts on marine microorganisms. *Nat commun* 9(1):1-15. <https://doi.org/10.1038/s41467-018-04970-7>
- Malerba ME, Marshall DJ, Palacios MM, Raven JA, Beardall J (2021) Cell size influences inorganic carbon acquisition in artificially selected phytoplankton. *New Phytol* 229:2647-2659. <https://doi.org/10.1111/nph.17068>

- Manimaran K, Karthikeyan P, Ashokkumar S, Prabu VA, Sampathkumar P (2012) Effect of copper on growth and enzyme activities of marine diatom, *Odontella mobiliensis*. Bull Environ Contam Toxicol 88(1):30-37. <https://doi.org/10.1007/s00128-011-0427-4>
- Marañón E (2015) Cell size as a key determinant of phytoplankton metabolism and community structure. Ann Rev Mar Sci 7:241-264. <https://doi.org/10.1146/annurev-marine-010814-015955>
- Masmoudi S, Nguyen-Deroche N, Caruso A, Ayadi H, Morant-Manceau A, Tremblin G (2013) Cadmium, copper, sodium and zinc effects on diatoms: from heaven to hell—a review. Cryptogam Algal 34(2):185-225. <https://doi.org/10.7872/crya.v34.iss2.2013.185>
- Mellett T, Brown MT, Chappell PD, Duckham C, Fitzsimmons JN, Till CP, Sherrell RM, Maldonado MT, Buck KN (2018) The biogeochemical cycling of iron, copper, nickel, cadmium, manganese, cobalt, lead, and scandium in a California Current experimental study. Limnol Oceanogr 63(S1):S425-S447. <https://doi.org/10.1002/lno.10751>
- Millero FJ, Woosley R, DiTrollo B, Waters J (2009) Effect of ocean acidification on the speciation of metals in seawater. Oceanography 22(4):72-85.
- Moffett JW, Dupont C (2007) Cu complexation by organic ligands in the sub-arctic NW Pacific and Bering Sea. Deep Sea Res Part I Oceanogr Res Pap 54(4):586-595. <https://doi.org/10.1016/j.dsr.2006.12.013>
- Moffett JW, Vedamati J, Goepfert TJ, Pratihary A, Gauns M, Naqvi SWA (2015) Biogeochemistry of iron in the Arabian Sea. Limnol Oceanogr 60(5):1671-1688. <https://doi.org/10.1002/lno.10132>
- Morel FM (2008) The co-evolution of phytoplankton and trace element cycles in the oceans. Geobiology 6(3):318-324. <https://doi.org/10.1111/j.1472-4669.2008.00144.x>
- Morin S, Lambert AS, Rodriguez EP, Dabrin A, Coquery M, Pesce S (2017) Changes in copper toxicity towards diatom communities with experimental warming. J Hazard Mater 334:223-232. <https://doi.org/10.1016/j.jhazmat.2017.04.016>
- Naqvi SWA, Sarma VVSS, Jayakumar DA (2002) Carbon cycling in the northern Arabian Sea during the northeast monsoon: Significance of salps. Mar Ecol Prog Ser 226:35-44. <https://doi.org/10.3354/meps226035>
- Narvekar J, D'Mello JR, Prasanna Kumar S, Banerjee P, Sharma V, Shenai-Tirodkar P (2017) Winter-time variability of the eastern Arabian Sea: A comparison between 2003 and 2013. Geophys Res Lett 44(12):6269-6277. <https://doi.org/10.1002/2017GL072965>
- Nguyen-Deroche TLN, Le TT, Bui TV, Rince Y, Tremblin G, Morant-Manceau A (2009) Effects of copper on growth and photosynthesis in marine diatoms: a comparison between species from two different geographical areas. Cryptogam Algal 30(2):97.
- Paasche E (1973) Silicon and the ecology of marine plankton diatoms. I. *Thalassiosira pseudonana* (*Cyclotella nana*) grown in a chemostat with silicate as limiting nutrient. Mar Biol 19(2):117-126.
- Paytan A, Mackey KR, Chen Y, Lima ID, Doney SC, Mahowald N, Labiosa R Post AF (2009) Toxicity of atmospheric aerosols on marine phytoplankton. PNAS 106(12):4601-4605. <https://doi.org/10.1073/pnas.0811486106>

- Pease PP, Tchakerian VP, Tindale NW (1998) Aerosols over the Arabian Sea: geochemistry and source areas for aeolian desert dust. *J Arid Environ* 39(3):477-496.
- Pierrot DE, Lewis E, Wallace DWR MS Excel program developed for CO₂ system calculations. Carbon Dioxide Information Analysis Center, Oak Ridge National Laboratory, US Department of Energy. ORNL/CDIAC-IOS, (2006).
- Raven J, Caldeira K, Elderfield H, Hoegh-Guldberg O, Liss P, Riebesell U, Watson A (2005) *Ocean acidification due to increasing atmospheric carbon dioxide*. The Royal Society.
- Raven JA (1987) The role of vacuoles. *New Phytol* 357-422.
- Rijstenbil JW, Derksen JWM, Gerringa LJA, Poortvliet TCW, Sandee A, Van den Berg M, Wijnholds JA (1994) Oxidative stress induced by copper: defense and damage in the marine planktonic diatom *Ditylum brightwellii*, grown in continuous cultures with high and low zinc levels. *Mar Biol* 119(4):583-590. <https://doi.org/10.1007/BF00354321>
- Rodushkin I, Ruth T (1997) Determination of trace metals in estuarine and sea-water reference materials by high resolution inductively coupled plasma mass spectrometry. *J Anal At Spectrom* 12(10):1181-1185.
- Rost B, Riebesell U, Burkhardt S, Sültemeyer D (2003) Carbon acquisition of bloom-forming marine phytoplankton. *Limnol Oceanogr* 48(1):55-67. <https://doi.org/10.4319/lo.2003.48.1.0055>
- Rueter Jr JG, Morel FM (1981) The interaction between zinc deficiency and copper toxicity as it affects the silicic acid uptake mechanisms in *Thalassiosira pseudonana* 1. *Limnol Oceanogr* 26(1):67-73.
- Sabine CL, Feely RA, Gruber N, Key RM, Lee K, Bullister JL, Rios AF (2004) The oceanic sink for anthropogenic CO₂. *Science* 305(5682):367-371. <https://doi.org/10.1126/science.1097403>
- Sarma VVSS (2003) Monthly variability in surface pCO₂ and net air-sea CO₂ flux in the Arabian Sea. *J Geophys Res Oceans* 108(C8). <https://doi.org/10.1029/2001JC001062>
- Sarma VVSS, Kumar MD, George MD (1998) The central and eastern Arabian Sea as a perennial source of atmospheric carbon dioxide. *Tellus B Chem Phys Meteorol* 50(2):179-184. <https://doi.org/10.3402/tellusb.v50i2.16095>
- Shaik AUR, Biswas H, Pal S (2017) Increased CO₂ availability promotes growth of a tropical coastal diatom assemblage (Goa coast, Arabian Sea, India). *Diatom Res* 32(3):325-339. <https://doi.org/10.1080/0269249X.2017.1379443>
- Sharma D, Biswas H, Bandyopadhyay D (2021) Simulated ocean acidification altered community composition and growth of a coastal phytoplankton assemblage (South West coast of India, eastern Arabian Sea). *Environ Sci Pollut Res* 1-18. <https://doi.org/10.1007/s11356-021-17141-x>
- Sharma D, Biswas H, Silori S, Bandyopadhyay D, Shaik AUR, Cardinal D, Ray D (2020) Impacts of Zn and Cu enrichment under ocean acidification scenario on a phytoplankton community from tropical upwelling system. *Mar Environ Res* 155:104880. <https://doi.org/10.1016/j.marenvres.2020.104880>

- Shetye SS, Kurian S, Naik H, Gauns M, Chndrasekhararao AV, Kumar A, Naik B (2019) Variability of organic nitrogen and its role in regulating phytoplankton in the eastern Arabian Sea. *Mar Pollut Bull* 141: 550-560. <https://doi.org/10.1016/j.marpolbul.2019.02.036>
- Shi D, Xu Y, Hopkinson BM, Morel FM (2010) Effect of ocean acidification on iron availability to marine phytoplankton. *Science* 327(5966):676-679. <https://doi.org/10.1126/science.1183517>
- Silva V, Marques CR, Campos I, Vidal T, Keizer JJ, Gonçalves F, Abrantes N (2018) Combined effect of copper sulfate and water temperature on key freshwater trophic levels—approaching potential climatic change scenarios. *Ecotox Environ Safe* 148:384-392. <https://doi.org/10.1016/j.ecoenv.2017.10.035>
- Stockdale A, Tipping E, Lofts S, Mortimer RJ (2016) Effect of ocean acidification on organic and inorganic speciation of trace metals. *Environ Sci Tech* 50(4):1906-1913. <https://doi.org/10.1021/acs.est.5b05624>
- Stoecker DK, Sunda WG, Davis LH (1986) Effects of copper and zinc on two planktonic ciliates. *Mar Biol* 92(1):21-29. <https://doi.org/10.1007/BF00392741>
- Sun J, Hutchins DA, Feng Y, Seubert EL, Caron DA, Fu FX (2011) Effects of changing $p\text{CO}_2$ and phosphate availability on domoic acid production and physiology of the marine harmful bloom diatom *Pseudo-nitzschia multiseries*. *Limnol Oceanogr* 56(3):829-840. <https://doi.org/10.4319/lo.2011.56.3.0829>
- Sunda WG (1989) Trace metal interactions with marine phytoplankton. *Biological Oceanography* 6(5-6):411-442.
- Sunda WG (2012) Feedback interactions between trace metal nutrients and phytoplankton in the ocean. *Front Microbiol* 3:204. <https://doi.org/10.3389/fmicb.2012.00204>
- Sunda WG, Huntsman SA (1986) Relationships among growth rate, cellular manganese concentrations and manganese transport kinetics in estuarine and oceanic species of the diatom *Thalassiosira*. *J Phycol* 22:259–270. <https://doi.org/10.1111/j.1529-8817.1986.tb00022.x>
- Takano S, Tanimizu M, Hirata T, Sohrin Y (2014) Isotopic constraints on biogeochemical cycling of copper in the ocean. *Nat Commun* 5(1):1-7. <https://doi.org/10.1038/ncomms6663>
- Tatters AO, Fu FX, Hutchins DA (2012) High CO_2 and silicate limitation synergistically increase the toxicity of *Pseudo-nitzschia fraudulenta*. *PloS one*, 7(2):32116. <https://doi.org/10.1371/journal.pone.0032116>
- Taucher J, Arístegui J, Bach LT, Guan W, Montero MF, Nauendorf A, Riebesell U (2018) Response of subtropical phytoplankton communities to ocean acidification under oligotrophic conditions and during nutrient fertilization. *Front Mar Sc* 5: 330. <https://doi.org/10.3389/fmars.2018.00330>
- Thimijan RW, Heins RD (1983) Photometric, radiometric, and quantum light units of measure: a review of procedures for interconversion. *Hort Science* 18:818-822.
- Tian HZ, Zhu CY, Gao JJ, Cheng K, Hao JM, Wang K, Zhou JR (2015) Quantitative assessment of atmospheric emissions of toxic heavy metals from anthropogenic sources in China: historical trend, spatial distribution, uncertainties, and control policies. *Atmos Chem Phys* 15(17):10127-10147. <https://doi.org/10.5194/acp-15-10127-2015>

- Tomas CR (Ed.) (1997) Identifying marine phytoplankton. Elsevier.
- Twining BS, Baines SB (2013) The trace metal composition of marine phytoplankton. *Ann Rev Mar Sci* 5:191-215. <https://doi.org/10.1146/annurev-marine-121211-172322>
- Uitz J, Claustre H, Morel A, Hooker SB (2006) Vertical distribution of phytoplankton communities in open ocean: An assessment based on surface chlorophyll. *J Geophys Res Oceans* 111(C8). <https://doi.org/10.1029/2005JC003207>
- UNESCO 1994. Knap AH, Michaels A, Close AR, Ducklow H, Dickson AG (1996) Protocols for the joint global ocean flux study (JGOFS) core measurements. *JGOFS*, Reprint of the IOC Manuals and Guides No. 29, 19.
- Valenzuela JJ, de Lomana ALG, Lee A, Armbrust EV, Orellana MV, Baliga NS (2018) Ocean acidification conditions increase resilience of marine diatoms. *Nat Commun* 9(1):1-10. <https://doi.org/10.1038/s41467-018-04742-3>
- Valsala V, Sreeush MG, Anju M, Sreenivas P, Tiwari YK, Chakraborty K, Sijikumar S (2021) An observing system simulation experiment for Indian Ocean surface $p\text{CO}_2$ measurements. *Prog Oceanogr* 194:102570. <https://doi.org/10.1016/j.pocean.2021.102570>
- Van Heukelem L, Thomas CS (2001) Computer-assisted high-performance liquid chromatography method development with applications to the isolation and analysis of phytoplankton pigments. *J Chromatogr A* 910(1):31-49. [https://doi.org/10.1016/S0378-4347\(00\)00603-4](https://doi.org/10.1016/S0378-4347(00)00603-4)
- Vidussi F, Claustre H, Manca BB, Luchetta A, Marty JC (2001) Phytoplankton pigment distribution in relation to upper thermocline circulation in the eastern Mediterranean Sea during winter. *J Geophys Res Oceans* 106(C9):19939-19956. <https://doi.org/10.1029/1999JC000308>
- Vijayan AK, Reddy BB, Sudheesh V, Marathe PH, Nampoothiri VN, Harikrishnachari NV, Kavya P, Gupta GVM, Ramanamurthy MV (2021) Phytoplankton community structure in a contrasting physico-chemical regime along the eastern Arabian Sea during the winter monsoon. *J Mar Sys* 215:103501. <https://doi.org/10.1016/j.jmarsys.2020.103501>
- Waldron KJ, Rutherford JC, Ford D, Robinson NJ (2009) Metalloproteins and metal sensing. *Nature*, 460(7257):823-830. <https://doi.org/10.1038/nature08300>
- Wang MJ, Wang WX (2008) Temperature-dependent sensitivity of a marine diatom to cadmium stress explained by subcellular distribution and thiol synthesis. *Enviro Sci Tech* 42(22):8603-8608. <https://doi.org/10.1021/es801470w>
- Wei Y, Zhu N, Lavoie M, Wang J, Qian H, Fu Z (2014) Copper toxicity to *Phaeodactylum tricornutum*: a survey of the sensitivity of various toxicity endpoints at the physiological, biochemical, molecular and structural levels. *Biometals*, 27(3):527-537.
- Wolf KK, Hoppe CJ, Rost B (2018) Resilience by diversity: Large intraspecific differences in climate change responses of an Arctic diatom. *Limnol Oceanogr* 63(1):397-411. <https://doi.org/10.1002/lno.10639>
- Wu Y, Campbell DA, Gao K (2017) Short-term elevated CO_2 exposure stimulated photochemical performance of a coastal marine diatom. *Mar Environ Res* 125:42-48. <https://doi.org/10.1016/j.marenvres.2016.12.001>

- Wu Y, Campbell DA, Irwin AJ, Suggett DJ, Finkel ZV (2014) Ocean acidification enhances the growth rate of larger diatoms. *Limnol Oceanogr* 59(3):1027-1034. <https://doi.org/10.4319/lo.2014.59.3.1027>
- Wu Y, Gao K, Riebesell U (2010) CO₂-induced seawater acidification affects physiological performance of the marine diatom *Phaeodactylum tricornutum*. *Biogeosciences* 7(9):2915-2923. <https://doi.org/10.5194/bg-7-2915-2010>
- Xu D, Schaum CE, Li B, Chen Y, Tong S, Fu FX, Hutchins DA, Zhang X, Fan X, Han W, Wang Y (2021) Acclimation and adaptation to elevated p CO₂ increase arsenic resilience in marine diatoms. *The ISME Journal* 1-15. <https://doi.org/10.1038/s41396-020-00873-y>
- Yang G, Gao K (2012) Physiological responses of the marine diatom *Thalassiosira pseudonana* to increased pCO₂ and seawater acidity. *Mar Environ Res* 79:142-151. <https://doi.org/10.1016/j.marenvres.2012.06.002>
- Yang T, Chen Y, Zhou S, Li H (2019) Impacts of aerosol copper on marine phytoplankton: A review. *Atmosphere* 10(7):414. <https://doi.org/10.3390/atmos10070414>
- Young JN, Kranz SA, Goldman JA, Tortell PD, Morel FM (2015) Antarctic phytoplankton down-regulate their carbon-concentrating mechanisms under high CO₂ with no change in growth rates. *Mar Ecol Prog Ser* 532: 13-28. <http://dx.doi.org/10.3354/meps11336>
- Yung MM, Kwok KW, Djurišić AB, Giesy JP, Leung KM (2017) Influences of temperature and salinity on physicochemical properties and toxicity of zinc oxide nanoparticles to the marine diatom *Thalassiosira pseudonana*. *Sci Rep* 7(1):1-9. <https://doi.org/10.1038/s41598-017-03889-1>
- Zhou B, Ma J, Chen F, Zou Y, Wei Y, Zhong H, Pan K (2020) Mechanisms underlying silicon-dependent metal tolerance in the marine diatom *Phaeodactylum tricornutum*. *Environ Poll* 262:114331. <https://doi.org/10.1016/j.envpol.2020.114331>

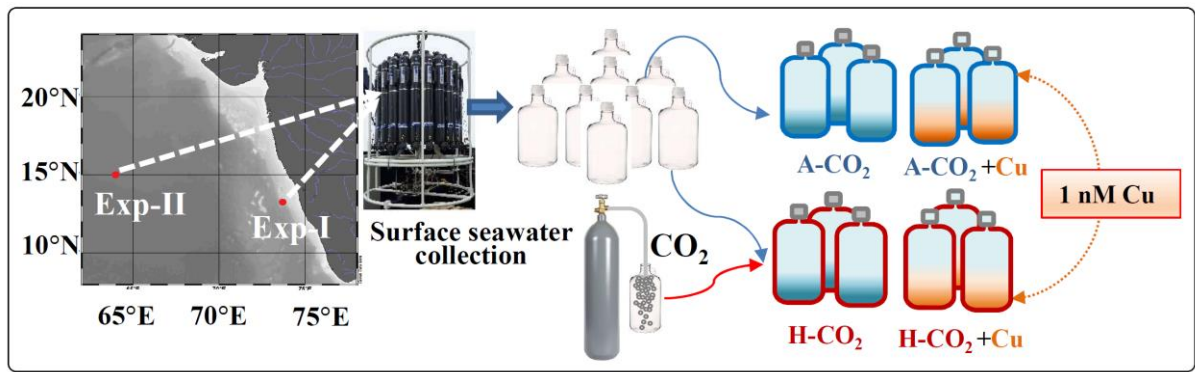


Figure 1: Map showing the surface seawater sampling locations in the southwestern shelf of India (Exp-I) and the central Arabian Sea (Exp-II) during the winter monsoon (Dec 2019). The schematic represents the experimental design.

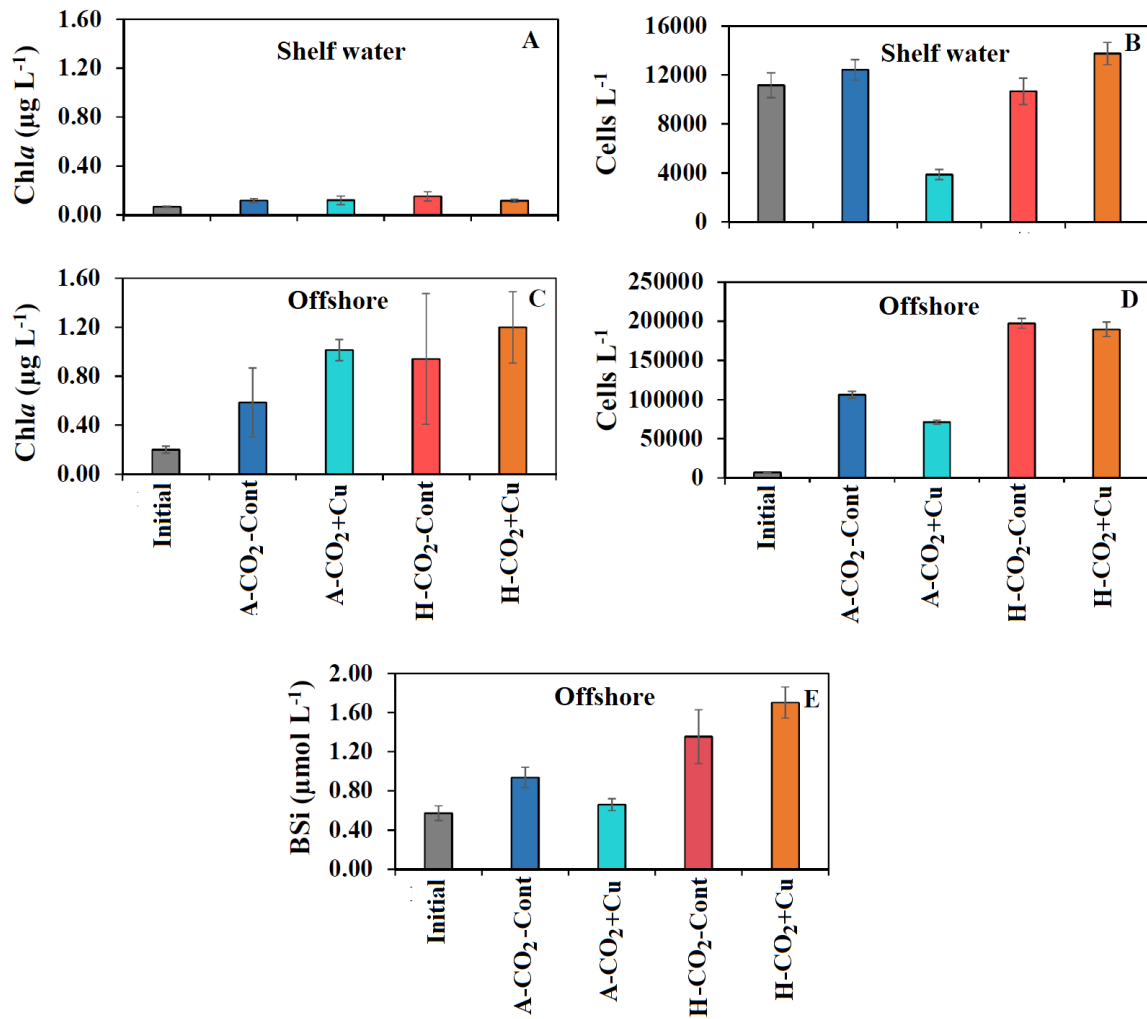


Figure 2: Chla concentrations (a); cell density (b) in Exp-I (A-CO₂ ≈420 µatm and H-CO₂ ≈1200 µatm; Chla contents (c); cell density (d) and BSi concentrations (e) in Exp-II (A-CO₂ ≈450 µatm and H-CO₂ ≈ 1100 µatm) (n =3; ±SD).

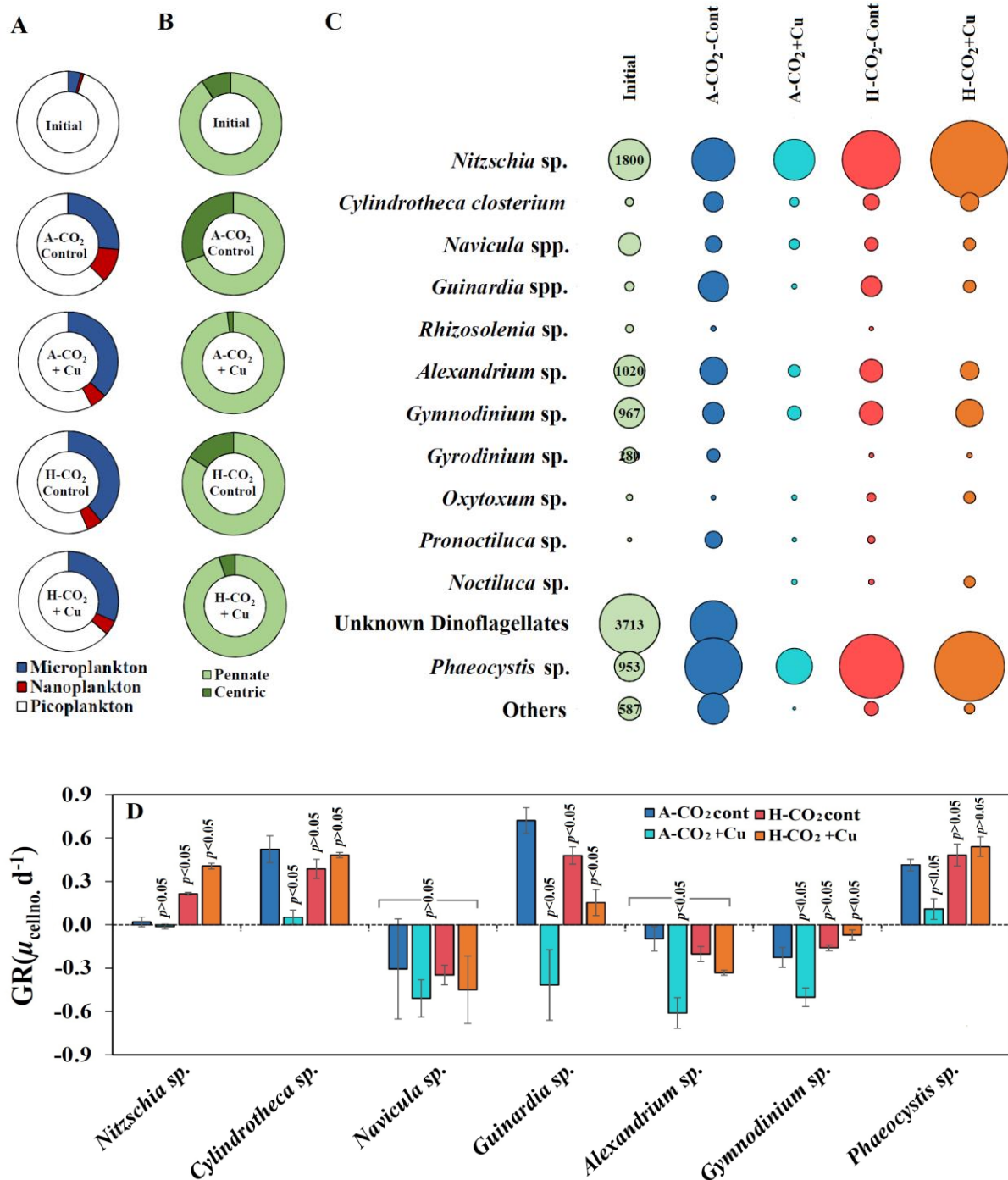


Figure 3: Relative contribution of different size classes of phytoplankton (micro, nano, and picophytoplankton) to total Chla calculated from diagnostic pigments (a); relative contribution (%) of centric and pennate diatom derived from microscopy (b); absolute cell density of the major phytoplankton species (c) analyzed by microscopy and species-specific GR growth rate [μ (d^{-1})] of the dominating phytoplankton species (d) in Exp-I. The p -values mentioned above the error bars indicate the level of significance concerning the impact of either high CO₂ or Cu compared to the controls ($n = 3$; \pm SD).

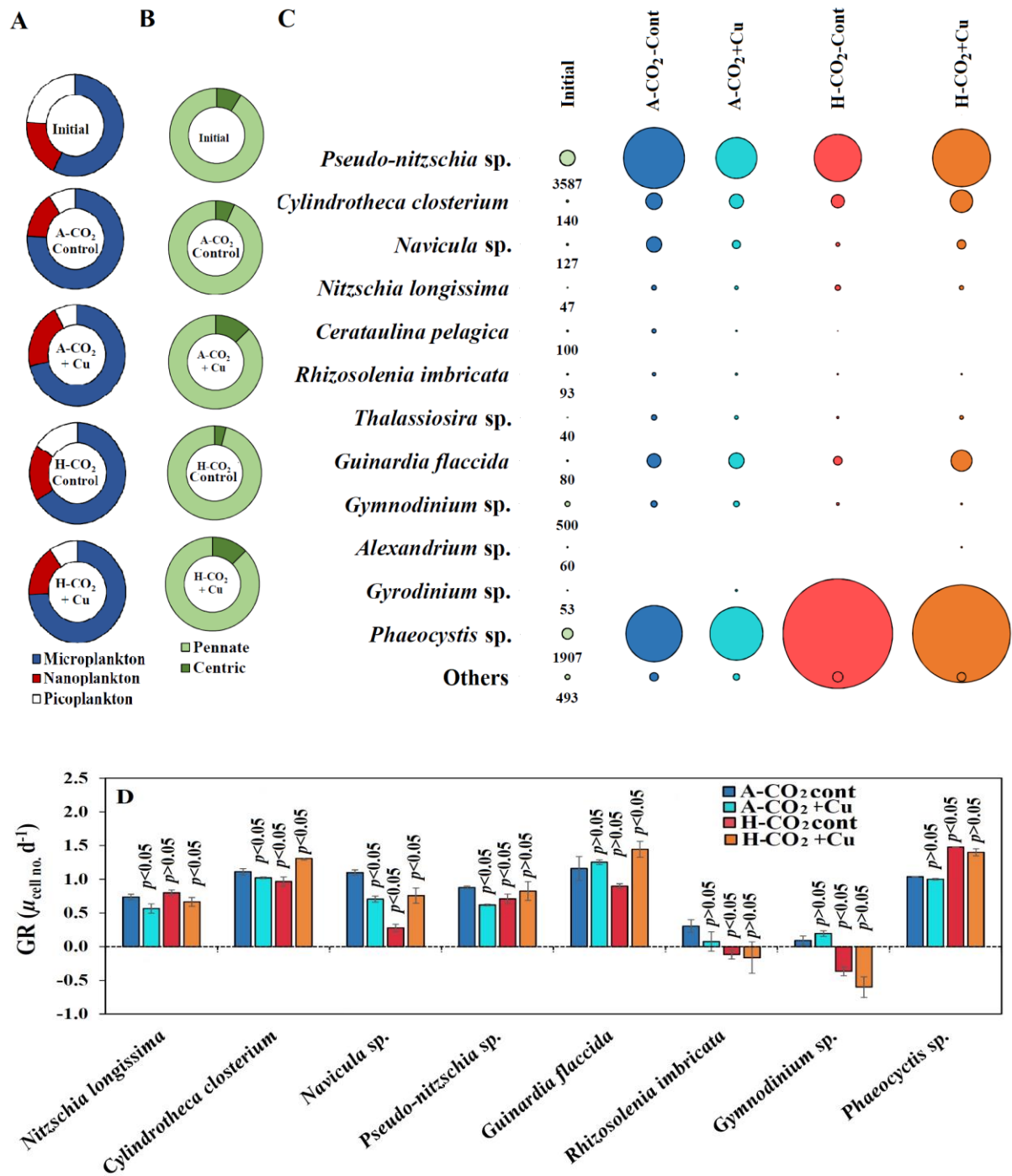


Figure 4: Relative contribution of different size classes of phytoplankton (micro, nano, and picophytoplankton) to total Chla calculated from diagnostic pigments (a); relative contribution (%) of centric and pennate diatom derived from microscopy (b); absolute cell density of the major phytoplankton species (c) analyzed by microscopy and species-specific growth rate [μ (d^{-1})] of the dominating phytoplankton species (d) in Exp-II. The p -values mentioned above the error bars indicate the level of significance concerning the impact of either high CO₂ or Cu compared to the controls ($n = 3; \pm\text{SD}$).

Table 1: The initial values of dissolved Cu levels and the carbon chemistry parameters during Exp-I and Exp-II (values \pm SD; $n = 3$). The TA and DIC values were used to calculate the $p\text{CO}_2$ and pH values using CO2SYS.

		$p\text{CO}_2$ (μatm)	pH (NBS)	TA ($\mu\text{mol kg}^{-1}$)	DIC ($\mu\text{mol kg}^{-1}$)	Dissolved Cu (nM)
Experiment-I	A-CO ₂	434 \pm 19	8.16 \pm 0.0 2	2283 \pm 10	1965 \pm 9	2.39 \pm 0.16
	H-CO ₂	1270 \pm 58	7.76 \pm 0.0 2		2161 \pm 7	
Experiment-II	A-CO ₂	456 \pm 3.6	8.14 \pm 0.0 03	2358 \pm 19	1995 \pm 18	1.82 \pm 0.39
	H-CO ₂	1100 \pm 47. 5	7.78 \pm 0.0 17		2196.7 \pm 2	

Table 2: The initial and final values of dissolved inorganic nutrients during Exp-I and Exp-II (values \pm SD; $n = 3$).

Experiment-I		Nitrate+nitrite	DIP	DSi
		($\mu\text{mol kg}^{-1}$)	($\mu\text{mol kg}^{-1}$)	($\mu\text{mol kg}^{-1}$)
Initial	A-CO ₂	0.22 \pm 0.02	0.1 \pm 0	1.55 \pm 0.05
	H-CO ₂			
Final	A-CO ₂	0.2 \pm 0	0.18 \pm 0.009	1.11 \pm 0.05
	A-CO ₂ +Cu	0.38 \pm 0.01	0.12 \pm 0.01	0.96 \pm 0.08
	H-CO ₂	0.45 \pm 0.12	0.12 \pm 0.009	1.32 \pm 0.15
	H-CO ₂ +Cu	0.36 \pm 0.16	0.13 \pm 0.009	1.19 \pm 0.08
Experiment-II				
Initial	A-CO ₂	3.28 \pm 0.03	0.37 \pm 0	1.95 \pm 0.07
	H-CO ₂			
Final	A-CO ₂	2.2 \pm 0.52	0.38 \pm 0.006	1.69 \pm 0.9
	A-CO ₂ +Cu	2.53 \pm 0.15	0.41 \pm 0.006	1.82 \pm 0.75
	H-CO ₂	2.44 \pm 0.63	0.39 \pm 0.04	1.09 \pm 0.17
	H-CO ₂ +Cu	2.08 \pm 0.30	0.39 \pm 0.006	0.76 \pm 0.11

Table 3: Individual phytoplankton cell density (L^{-1}) and relative abundance (%) calculated from the microscopic analysis for Exp-I ($n = 3$; \pm SD).

Phytoplankton species	Initial		A-CO ₂		A-CO ₂ + Cu		H-CO ₂		H-CO ₂ + Cu	
	Cell density	RA (%)	Cell density	RA (%)	Cell density	RA (%)	Cell density	RA (%)	Cell density	RA (%)
<i>Nitzschia</i> sp.	1800 \pm 471	17	1915 \pm 187	15.95	1738 \pm 85	46.07	3431 \pm 93	33.78	6080 \pm 359	45.63
<i>Cylindrotheca closterium</i>	86.67 \pm 9.4	0.82	427 \pm 127	3.58	102 \pm 15	2.68	280 \pm 58	2.78	369 \pm 20	2.77
<i>Navicula</i> spp.	546.7 \pm 37	5.22	289 \pm 199	2.36	124 \pm 46	3.24	196 \pm 41	1.94	164 \pm 100	1.20
<i>Rhizosolenia</i> sp.	80 \pm 56	0.74	35 \pm 15	0.30	-	-	26.6 \pm 0	0.26	-	-
<i>Guinardia</i> spp.	106.7 \pm 113	0.98	951 \pm 265	7.82	36 \pm 20	0.91	453 \pm 80	4.48	173 \pm 48	1.32
<i>Eucampia</i> sp.	20 \pm 9.4	0.19	20 \pm 9.4	0.17	-	-	-	-	53.3 \pm 0	0.37
<i>Thalassiosira</i> sp.	6.7 \pm 9	0.07	-	0.12	-	-	-	-	-	-
<i>Pseudo-nitzschia</i> sp.	253.3 \pm 38	2.43	84 \pm 38	0.72	-	-	-	-	-	-
<i>Coscinodiscus</i> sp.	13.3 \pm 0	0.13	58 \pm 43	0.47	-	-	44 \pm 15	0.44	20 \pm 9.4	0.15
<i>Chaetoceros</i> sp.	40 \pm 0	0.18	133.3 \pm 13	1.12	-	-	31 \pm 7	0.31	115 \pm 31	0.87
<i>Asteromphalus</i> sp.	106.7 \pm 0	0.48	33 \pm 28	0.29	-	-	-	-	-	-
<i>Hamiaulus</i> sp.	13.3 \pm 0	0.13	-	-	-	-	-	-	-	-
<i>Leptocylindrus</i> spp.	-	-	-	-	-	-	209 \pm 33	2.05	53.3 \pm 0	0.42
<i>Pheocystis</i> sp.	953 \pm 198	9.02	3311 \pm 404	27	1342 \pm 294	35	4124 \pm 963	40	4889 \pm 943	36.44
<i>Alexandrium</i> sp.	1020 \pm 348	9.60	778 \pm 185	6.44	169 \pm 54	4.37	560 \pm 92	5.46	378 \pm 20	2.83

<i>Gymnodinium</i> sp.	966.7±160	9.16	498±96	4.14	218±41	5.71	600±35	5.91	782±85	5.90
<i>Gyrodinium</i> sp.	280±94	2.64	187±58	1.57	-	-	31±20	0.29	36±15	0.26
<i>Protoperidinium sternii</i>	66.7±19	0.64	53±35	0.44	-	-	31±20	0.29	-	-
<i>Oxytoxum</i> sp.	53.3±56	0.53	31±7	0.26	36±20	0.92	93±35	0.92	156±47	1.19
<i>Pyrodinium</i> sp.	40±38	0.39	-	-	-	-	-	-	-	-
<i>Trichodesmium</i> sp.	80±38	0.75	22±7.7	0.18	-	-	33±9.4	0.35	-	-
<i>Amphiprora</i> sp.	13.3±0	0.12	13.3±0	0.06	-	-	-	-	-	-
<i>Prorocentrum</i> sp.	13.3±0	0.13	-	-	-	-	-	-	-	-
<i>Krenia</i> sp.	26.7±0	0.24	-	-	-	-	-	-	-	-
<i>Dinophysis</i> sp.	13.3±0	0.07	-	-	-	-	-	-	-	-
<i>Pronoctiluca</i> sp.	26.7±19	0.26	307±128	0.11	26.6±0	0.7	66±13	0.65	-	-
<i>Noctiluca</i> sp.	-	-	-	-	40±0	0.95	40±19	0.40	147±40	1.09
Unknown	3713.3±216	35.46	2222±96	19	-	-	-	-	-	-
Dinoflagellates										
<i>Dictyocha fibula</i>	13.3±0	0.13	13.3±0	0.10	-	-	-	-	-	-

Table 4: Individual phytoplankton cell density (L^{-1}) and relative abundance (%) calculated from the microscopic analysis for Exp-II ($n = 3$; \pm SD).

Phytoplankton species	Initial		A-CO ₂		A-CO ₂ + Cu		H-CO ₂		H-CO ₂ + Cu	
	Cell density	RA (%)	Cell density	RA (%)	Cell density	RA (%)	Cell density	RA (%)	Cell density	RA (%)
<i>Pseudo-nitzschia</i> sp.	3586.6 \pm 170	50.39	49991 \pm 2927	47	22933 \pm 908	32	30560 \pm 6490	15	45022 \pm 18495	24
<i>Cylindrotheca closterium</i>	140 \pm 9.4	1.97	3964 \pm 549	3.7	2987 \pm 116	4.20	2578 \pm 537	1.3	7129 \pm 503	3.7
<i>Nitzschia longissima</i>	46.6 \pm 9.4	0.66	426 \pm 53	0.4	258 \pm 55	0.36	516 \pm 67	0.26	347 \pm 71	0.18
<i>Nitzschia</i> sp.	-	-	613 \pm 192	0.58	524 \pm 81	0.7	969 \pm 484	0.5	266.6 \pm 38	0.13
<i>Navicula</i> sp.	126.6 \pm 28	1.79	3440 \pm 419	3.3	1057 \pm 136	1.49	293 \pm 46	0.15	1271 \pm 401	0.67
<i>Rhizosolenia imbricata</i>	93.3 \pm 57	1.34	240 \pm 71	0.23	124 \pm 55	0.18	66.6 \pm 19	0.03	67 \pm 56	0.03
<i>Chaetoceros</i> sp.	13.3 \pm 0	0.19	-	-	-	-	-	-	40 \pm 19	0.02
<i>Guinardia flaccida</i>	80 \pm 38	1.11	2836 \pm 1440	2.63	3449 \pm 362	4.8	1182 \pm 123	0.6	6347 \pm 2060	3.4

<i>Cerataulina pelagica</i>	100±28	1.40	356±55	0.36	71±40	0.1	26.6±0	0.01	-	-
<i>Cosinodiscus</i> sp.	26.6±19	0.38	80±0	0.07	-	-	53.3±0	0.03	-	-
<i>Thalassiosira</i> sp.	40±0	0.54	507±71	0.5	284±61	0.4	120±0	0.06	280±57	0.15
<i>Gyrosigma</i> sp.	53.3±0	0.72	89±31	0.08	-	-	-	-	169±31	0.10
<i>Leptocylindrus</i> sp.	93.3±0	1.26	124±67	0.12	98±40	0.14	-	-	187±71	0.1
<i>Phaeocystis</i> sp.	1906.6±7	26.8	42889±3	40.4	38364±1	54	160427	81	127946±20	67
	5		88		382		±1425		667	
<i>Gymnodinium</i> sp	500±141	6.98	667±141	0.63	764±200	1.1	169±31	0.09	89±41	0.05
<i>Protoperidinium</i> sp.	13.3±0	0.19	-	-	-	-	-	-	-	-
<i>Alexandrium</i> sp.	60±28	0.86	-	-	-	-	-	-	71±40	0.04
<i>Gyrodinium</i> sp.	33.3±28	0.46	-	-	116±40	0.2	-	-	-	-
<i>Oxytoxum</i> sp.	-	-	26.6±0	0.03	-	-	-	-	-	-
<i>Pronoctiluca</i> sp.	120±75	1.6	106.6±0	0.10	-	-	-	-	-	-